

1 History of Superconductivity: Conventional, High-Transition Temperature and Novel Superconductors

K. H. Bennemann Dept. of Physics, Freie Universität Berlin, Germany

J. B. Ketterson Dept. of Physics and Astronomy, Northwestern University, Evanston, USA

1.1 Introduction	3
1.2 Novel Superconductors	9
1.3 Granular Superconductors, Mesoscopic Systems, Josephson Junctions	18
1.4 Outlook	23
References	25

1.1 Introduction

Since its discovery by H. Kamerlingh Onnes in Leiden [1] almost 100 years ago, superconductivity has remained an important area of solid state physics with continuing surprises. Its first observation in Hg, illustrated for historical reasons in Fig. 1.1, resulted from general advances in low temperature physics (liquefying He). The important continuing discovery

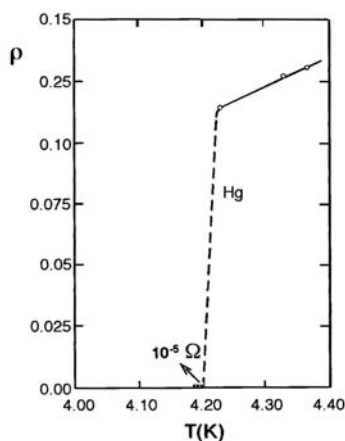


Fig. 1.1. Illustration of Kamerlingh Onnes' discovery of superconductivity and vanishing of the electrical resistivity ρ in 1911

of new superconductors resulted from advances in material science physics. By 1980 superconductivity had been observed in many metals and alloys thereof. For an illustration see Fig. 1.2 [2]. Remarkably, the classical ferromagnets like Ni, Fe, etc. did not exhibit superconductivity. Only for the non-magnetic state and under (strong) pressure has superconductivity been reported (for example in iron, $T_c = 2$ K) [3]. From the beginning a strong motivation was to find superconductors with a high transition temperature T_c . However, until about 1980 the A-15 compound Nb_3Ge remained the superconductor with the highest T_c at about 30 K, see Fig. 1.3. In order to achieve higher T_c values also many alloys and the effect of applying pressure were studied.

Soon after 1980 exciting new superconductors belonging to rather different material classes were discovered. The situation including the high T_c cuprate superconductors discovered by Bednorz and Müller [4] in 1986 is illustrated in Fig. 1.4. For several reasons this tremendously stimulated the minds of the physics community. High- T_c cuprate superconductivity exhibited puzzling new behavior. Perhaps this helped the birth of new surprises which were yet to come.

One may note that the history of superconductivity exhibits similar alternating periods of great ex-

H																	He
Li	Be											B	C	N	O	F	Ne
Na	Mg											Al	Si	P	S	Cl	Ar
K	Ca	Sc	Ti	V	Cr	Mn	Fe	Co	Ni	Cu	Zn	Ga	Ge	As	Se	Br	Kr
Rb	Sr	Y	Zr	Nb	Mo	Tc	Ru	Rh	Pd	Ag	Cd	In	Sn	Sb	Te	J	Xe
Cs	Ba	La	Hf	Ta	W	Re	Os	Ir	Pt	Au	Hg	Tl	Pb	Bi	Po	At	Rn
Fr	Ra	Ac	Ce	Pr	Nd	Pm	Sm	Eu	Gd	Tb	Dy	Ho	Er	Tm	Yb	Lu	
			Th	Pa	U	Np	Pu	Am	Cm	Bk	Cf	Es	Fm	Md	No	Lw	

Fig. 1.2. Overview of superconducting metals (blue) in the periodic table. Note the absence of superconductivity in the ferromagnetic transition metals and rare-earth and actinide metals. Other superconductors (under pressure) are marked in red. The superconducting transition temperature T_c is indicated

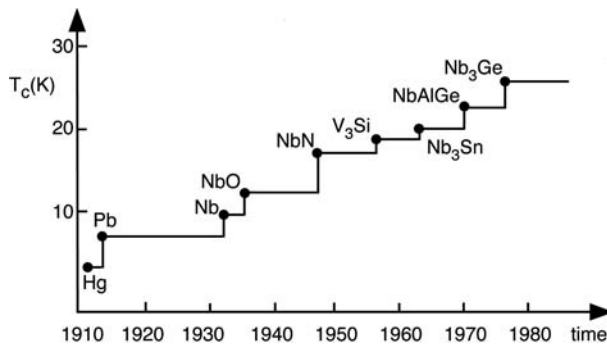


Fig. 1.3. History of the transition temperature T_c for the first 70 years following the discovery of superconductivity in 1911. The A-15 compounds were of particular interest in the search for higher T_c -superconductors

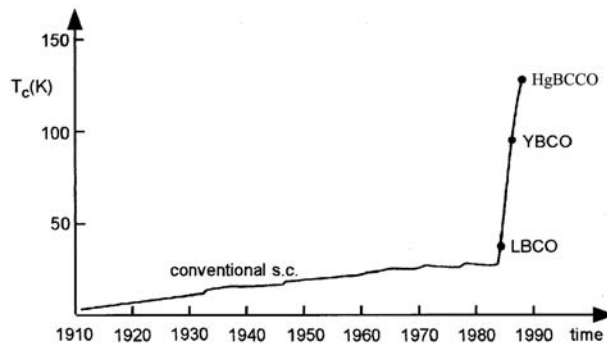


Fig. 1.4. High- T_c cuprate superconductors discovered by Bednorz and Müller in 1986. For $\text{La}_{2-x}\text{Ba}_x\text{CuO}_4$ a $T_c \simeq 35$ K, for $\text{YBa}_2\text{Cu}_3\text{O}_{7-\delta}$ a $T_c = 92$ K, and for $\text{HgBa}_2\text{Ca}_2\text{Cu}_3\text{O}_{8+\delta}$ a $T_c = 133$ K was observed, for example

citement and phases that were more quiet, as was the case for other important classical problems in physics. Generally, the study of superconductivity was a motor for new experimental techniques as well as for methods in theoretical physics, in many-body physics and quantum field theory, and was responsi-

ble for new concepts of quite general significance in physics. The noticeable interplay of experiment and theory was particularly fruitful as history shows, in particular regarding the electronic mechanism for phonon-mediated superconductivity and the symmetry of the superconducting state.

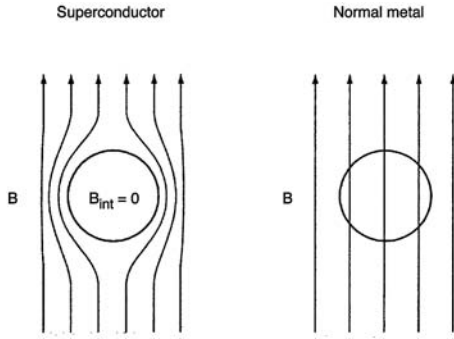


Fig. 1.5. Meissner effect for type I superconductors: If a superconductor in an external magnetic field H is cooled below its superconducting transition temperature T_c , the magnetic flux B is abruptly expelled. For particular values of B it penetrates the superconductor only within the penetration depth λ at the surface ($B = H + 4\pi M$)

Cornerstones in the early history of superconductivity were:

1. Observation of vanishing resistivity $\rho(R)$ at a critical temperature $T_c \simeq 4.2$ K in Hg by Kamerlingh Onnes [1] in 1911.
2. Observation of the diamagnetic behavior of type I superconductors by Meissner and Ochsenfeld in 1933, which opened the way towards a deeper understanding of superconductivity; see Fig. 1.5 for an illustration of the Meissner effect [5].
3. The London theory in 1935, which described the Meissner effect flux repulsion, by using for the superconducting current driven by the vector potential A the formula [6]

$$\mathbf{j}_s = - (c/4\pi\lambda_L^2) \mathbf{A}, \quad (1.1)$$

with $\lambda_L = (mc^2/4\pi e^2 n_s)^{1/2}$, and n_s the density of the superfluid. Then, from $\text{rot} \mathbf{j}_s$ and the Maxwell equations one gets the Meissner effect (see $(4\pi/c)\text{rot} \mathbf{j}_s = \nabla \times \nabla \times \mathbf{B}$).

4. The Isotope effect [7], $T_c \propto M^{-\alpha}$, $\alpha \approx 0.5$ for Hg, observed by Maxwell 1950 and which suggested that the electron–phonon coupling might be responsible for superconductivity.
5. The Ginzburg–Landau theory in 1950, which extended the London theory and introduced the order parameter [8]

$$\psi(\mathbf{r}, t) = |\psi| e^{i\varphi(\mathbf{r})}, \quad (1.2)$$

with $n_s \propto |\psi|^2$ and

$$\begin{aligned} \mathbf{j}_s &= 2e |\psi|^2 \mathbf{v}_s \\ &= \frac{2e\hbar}{m^*} |\psi|^2 \left(\nabla\varphi - \frac{2e}{\hbar c} \mathbf{A} \right). \end{aligned} \quad (1.3)$$

6. The breakthrough by the famous and most elegant theory of Bardeen, Cooper, Schrieffer (BCS) in 1956 which after almost 45 years gave a definite electronic explanation of superconductivity in terms of Cooper pairs ($\mathbf{k} \uparrow, -\mathbf{k} \downarrow$) forming in an energy shell $\hbar\omega_D$ (ω_D denotes the Debye frequency) around the Fermi energy ϵ_F resulting from the electron–phonon interaction [9].

The BCS theory became one of the most elegant and successful theories in physics [9]. It was further completed by the field theoretical approaches of Gor'kov [10], Abrikosov and Gor'kov [11], and Eliashberg [12]. Important in understanding (magnetic) field-dependence was Abrikosov's analysis based on the Ginzburg–Landau theory of type I superconductors ($\kappa < 1/\sqrt{2}$, $\kappa \equiv \lambda/\xi$, λ is the penetration depth, ξ the coherence length referring to the stiffness of ψ) and type II ones ($\kappa > 1/\sqrt{2}$), which allow magnetic flux ϕ to penetrate the superconductor in a regular array, quantized in units of the elementary flux quantum $\phi_0 = hc/2e$ [13]. Important was also the observation of flux quantization in a ring, flux $\phi = (n + \frac{1}{2})\frac{hc}{e}$, ($n = 0, \pm 1, \dots$), by Doll and N  bauer, and Deaver and Fairbank [16]. This is illustrated in Fig. 1.6.

A further step was Josephson's tunneling theory in 1962 describing also tunneling of Cooper pairs through a barrier between two superconductors [14]. The current is given by $j(t) = j_0 + \Delta j(\Delta\varphi)$, where $\Delta\varphi = \varphi_2 - \varphi_1$ is the phase difference between the two superconductors 1 and 2 separated by a tunnel barrier ($\Delta\varphi = \varphi_2^0 - \varphi_1^0 - (2e\hbar c) \int_1^2 dx A_x$). Then one may get for the Cooper pair current ($A = 0$ and voltage V)

$$\begin{aligned} j(t) &= j_0 + j_1 \sin \left(\varphi_2^0 - \varphi_1^0 - \frac{2e}{\hbar} V_{21} t \right), \\ \left(V_{21} = \frac{\hbar}{2e} \dot{\varphi}_{21} \right). \end{aligned} \quad (1.4)$$

Very important was also the study of the tunneling density of states by Schrieffer, Scalapino and Wilkens

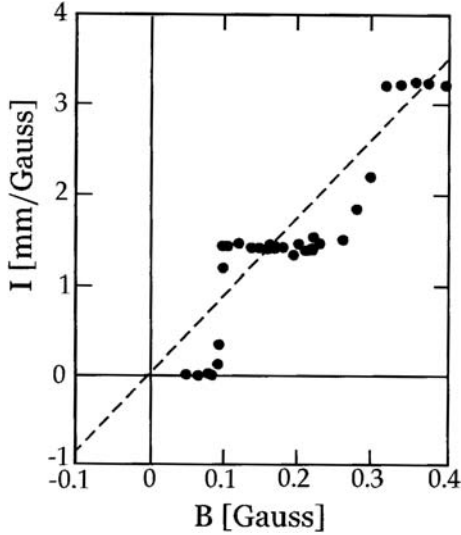


Fig. 1.6. Illustration of flux quantization in a superconducting Pb-cylinder. The signal I is proportional to the flux and B denotes the frozen-in field

in 1963 explaining observed detailed structure in the tunneling current and superconducting order parameter $\Delta(\omega)$ as due to the electron-phonon coupling ($N_T(\omega) = N(\epsilon_F) \text{Re} [\omega / \sqrt{\omega^2 - \Delta^2(\omega)}]$) [15]. It seemed that the electronic theory for superconductivity, which had replaced largely the early phenomenological theories by Casimir, Gorter (two-fluid model for n_s, n_n), by London for the Meissner effect and by Ginzburg-Landau, was largely completed.

The thermodynamical and electrodynamical behavior of type I superconductors for which the Meissner effect holds up to the critical magnetic field H_c and type II superconductors with magnetic flux penetration below B_{c2} and Meissner effect below B_{c1} was characterized by the influence of external fields on the Cooper pairs and the phase diagrams $T_c(B(T))$ and $T_c(j, B)$. Typical results are shown in Fig. 1.7. Clearly this behavior also sheds light on the interdependence of superconductivity and magnetism. Metals with parallel magnetic and superconducting activity are of central interest. Triplet Cooper pairing relates such superconductors intimately to superfluid ^3He . Superconductors with quantum-critical points are of special interest with respect to basic questions of quantum mechanics.

The search for superconductors with higher transition temperatures, see Fig. 1.3, became increasingly important. In this regard of particular interest was the work by McMillan [17], which attempted to relate T_c ,

$$T_c \propto \langle \omega_{ph} \rangle \exp\{-1/(\lambda - \mu^*)\}, \quad (1.5)$$

to characteristic parameters of the superconducting metals like electron-phonon coupling g or λ , electronic density of states at ϵ_F , etc. (λ is the electron-phonon coupling constant, $\lambda = 2 \int_0^\infty \frac{\alpha^2 F(\omega)}{\omega} d\omega$ with $F(\omega)$ characterizing the phonon spectrum). μ^* refers to the renormalized effective Coulomb interaction between the Cooper pairs forming electrons. For a

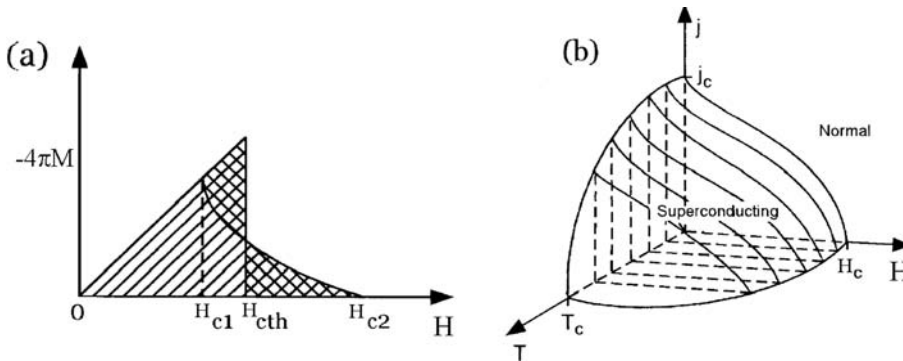


Fig. 1.7. Typical behavior of superconductors in an external magnetic field H : (a) type II superconductors with critical fields H_{c2} , below which flux penetrates, H_{c1} , below which perfect Meissner effect behavior occurs (magnetization M), (b) dependence on H and current j of type I superconductivity ($B = H + 4\pi M$)

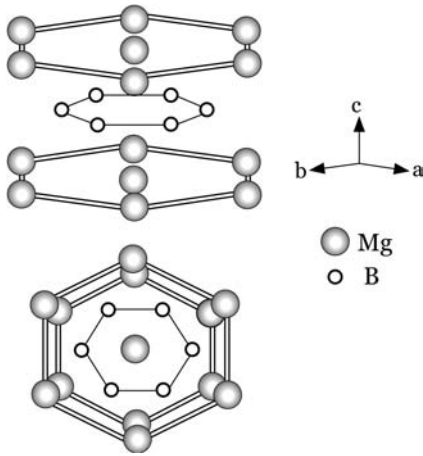


Fig. 1.8. Structure of MgB_2 (AlB_2 , etc.). The boron planes seem to play an important role regarding superconductivity and Cooper pairing. Note that the Mg-B bonds are softer than the B-B ones

long time one observed only superconductivity due to the electron-phonon coupling and that the A-15 compounds like V_3Si , Nb_3Ge , etc. had the highest T_c . The superconducting order parameter $\psi(\mathbf{r}, t)$ had s -wave symmetry. The prospects for finding superconductors with higher T_c was somewhat guided (and affected) by the estimates of a maximal T_c given by P.W. Anderson, Cohen, and Allen and others [18]. However, one expected that for increasing electron-phonon coupling strength λ , the resulting lattice instability limited essentially the occurrence of superconductivity ($T_c < T_c^{\text{max}}$).

In view of this the recent discovery of the type II superconductor MgB_2 with $T_c \simeq 40\text{K}$ and quasi two gaps, $\Delta_1 \simeq 4\text{ meV}$ and $\Delta_2 \simeq 7.5\text{ meV}$ due to π - and σ -type electrons was very remarkable. Both gaps have s -symmetry and result from the highly anisotropic layer-structure of the MgB_2 -lattice. Note, boron planes consisting of hexagon-B-rings characterize the structure, see Fig. 1.8. The dominating bonds of π -type and σ -type coupling to phonons causes superconductivity. As a consequence of the anisotropy one gets critical magnetic fields H_{c2}^{\parallel} and H_{c2}^{\perp} . One estimates $H_{c2}^{\perp} \sim (\xi^{\parallel})^{-2} \sim 0.2 H_{c2}^{\parallel}$. Here the H_{c2}^{\parallel} and H_{c2}^{\perp} refer to in-plane and perpendicular to B-plane upper critical field, respectively. Note that $H_{c2} \simeq \Phi_0 / \pi \xi^2$, $\xi \sim \Delta^{-1}$, Φ_0 refers to the elementary flux quantum. In Fig. 1.9 we illustrate the anisotropic behaviour of $H_{c2}(T)$ indicative of two gaps. It is interesting that MgB_2 can carry relatively strong superconducting currents in magnetic fields up to 3 T, which compares with that observed for high- T_c cuprates. Note the isotope effect as well as tunnel spectroscopy support phonon driven superconductivity. One gets that $\text{Mg}^{11} \rightarrow \text{Mg}^{10}$ increases T_c by about 1 K in accordance with $T_c \propto (\text{Mg})^{-1/2}$. Interestingly AlB_2 is not superconducting. Note that MgB_2 is another example of the interesting role played by the lattice structure regarding superconductivity.

Over the years many interesting studies of coexistence of superconductivity and magnetism (for example, the transition metals and their alloys, rare

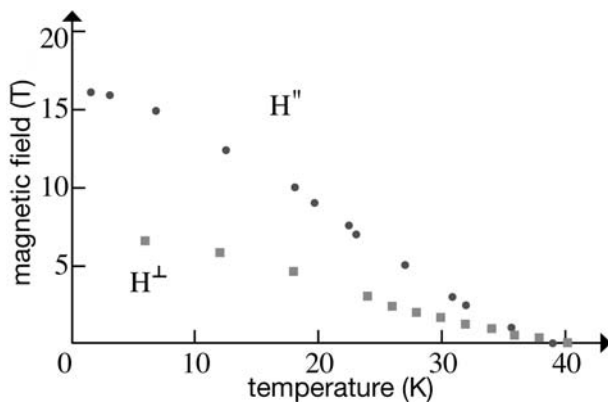


Fig. 1.9. Critical upper magnetic fields $H''(T)$ and $H_{c2}^{\perp}(T)$ referring to the B-planes and directions perpendicular to it, respectively, in the layered structure of MgB_2 . The anisotropic behavior of $H_{c2}(T)$ is indicative of the approximate two-gap behavior

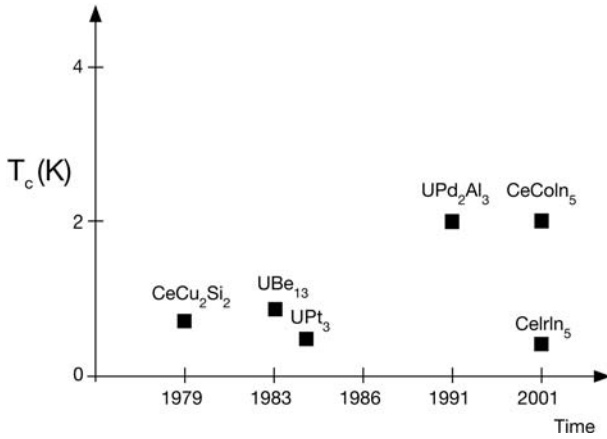


Fig. 1.10. Superconductivity in heavy-fermion metals

earth (RE) compounds, etc.) and of occurrence of superconductivity in metals with strongly correlated electrons and local spins were carried out (see, for example, the heavy-fermion systems in Fig. 1.10). That singlet Cooper pairs ($\mathbf{k} \uparrow, -\mathbf{k} \downarrow$) respond sensitively to magnetism and correlation was, of course, expected on general grounds, in view of the results shown in Fig. 1.2 and of the thermodynamical behavior in an external magnetic field (see Fig. 1.7 for illustration).

The studies of the effect of magnetism and magnetic fields were important for our understanding of superconductivity (for strongly renormalized quasiparticles, for polaronic type superconductivity, for Bose-Einstein vs. BCS type pair-condensation, etc.) and in particular for the search of superconductivity with the Cooper pair wave function

$$\psi(\mathbf{r}, t) = |\psi(\mathbf{r}, t)| e^{i\varphi(\mathbf{r}, t)} \quad (1.6)$$

having non-*s*-wave symmetry, describing triplet pairing, and pairing resulting not from electron-phonon interaction. Here, the discovery by Osheroff et al. [19] in 1972 observing spin-triplet pairing in superfluid ^3He , another Fermi-liquid besides the superconducting metals, was very important for the further history of superconductivity. Also, the study by Berk and Schrieffer in 1966 of the interdependence of superconductivity and spin-fluctuations prepared the development of new perspectives and for new research routes [20]. In this context experimental studies of superconductivity in UPt_3 , CeIn_3 ,

CePd_2Si_2 , $\text{U}_{1-x}\text{M}_x\text{Pd}_2\text{Al}_3$, ($\text{M} = \text{Y}, \text{Th}$, etc.), exhibiting spin-excitations, were important [21]. Recent experimental studies of the magnetically active intermetallic compound UGe_2 , of MgCNi_3 ($T_c = 8\text{K}$), of the magnetic organometallic compound $(\text{BETS})_2\text{FeCl}_4$ (where superconductivity is induced by a strong external magnetic field) and similar systems, for example, clearly indicate the interdependence of magnetism and superconductivity.

To illustrate the exciting new observations regarding the interplay of superconductivity and magnetism we show typical phase diagrams. In Fig. 1.11 we present results for UGe_2 . Further studies should reveal the mechanism for Cooper pairing (triplet versus singlet pairing), magnetic activity and electronic

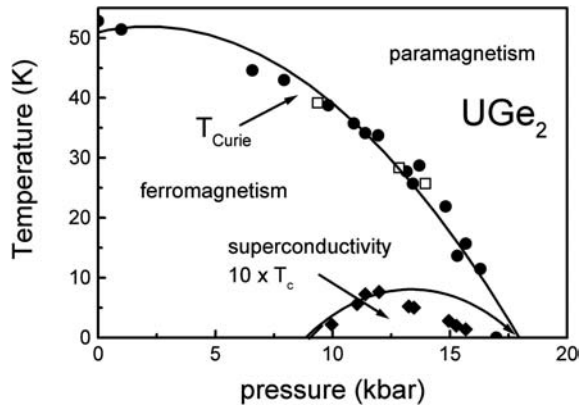


Fig. 1.11. Phase diagram of UGe_2

structure in the superconducting phase with relatively low T_c . Note, the behavior of $T_c(p)$. First T_c increases with pressure p , but then decreases again, and $T_c \rightarrow 0$ for $p \approx 17$ kbar.

Another compound with interesting magnetic and superconducting properties is ZrZn_2 , which exhibits itinerant ferromagnetism. It seems that superconductivity exists up to 22 kbar, but not in the paramagnetic phase. The formation and character of the Cooper pairs (triplet pairing?) must still be studied. One can expect that there may be many compounds with an interesting interdependence of superconductivity and magnetism.

In Fig. 1.12 we show the interesting results for iron (Fe) under pressure. It is remarkable that Fe becomes superconducting at low temperatures and for pressure between 15 and 30 GPa in the non-magnetic hexagonal-close-packed ϵ -phase. The Cooper pairing needs to be studied as well as important properties revealing the electronic basis of the phase diagram.

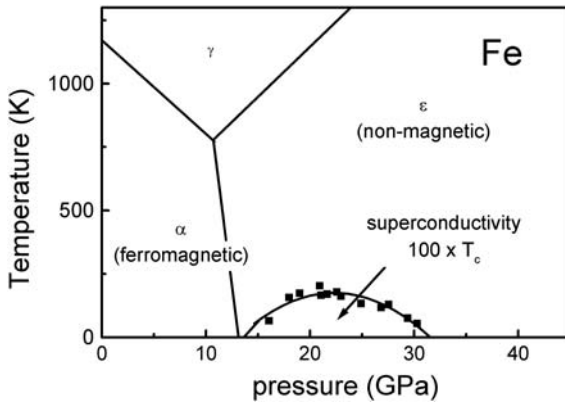


Fig. 1.12. Superconducting hexagonal ϵ -phase Fe under strong pressure. α, β, ϵ refers to the various Fe phases

In all conventional superconductors phase coherent Cooper pairing occurs at the transition-temperature T_c . The structure of the order parameter $\Delta_k(\omega)$, seen in the spectral-density, for example, for conventional superconductors reflects characteristic phonon frequencies involved in Cooper pairing. The Meissner effect occurs at T_c for phase coherent Cooper pairs. Also, in conventional superconductors typically non-magnetic impurities reduce T_c rela-

tively weakly, while paramagnetic impurities have a strong destructive effect and may destroy superconductivity. External magnetic fields and electrical currents destroy the superconducting state, break up Cooper pairs, and may even cause gapless superconductivity.

1.2 Novel Superconductors

(a) Cuprates (High-Transition Temperature Superconductors)

The superconductivity research changed dramatically when the high T_c -cuprate superconductors with CuO_2 -layers like $\text{La}_{2-x}\text{Sr}_x\text{CuO}_4$, $\text{YBa}_2\text{Cu}_3\text{O}_{7-\delta}$, $\text{Tl}_2\text{Ba}_2\text{CaCu}_2\text{O}_8$, etc. were discovered by Bednorz and Müller in 1986 with transition temperatures ranging from $T_c \simeq 35$ K to $T_c \simeq 160$ K (under pressure) in $\text{HgBa}_2\text{CaCu}_2\text{O}_{6+\delta}$ [4]. The carriers in the cuprates, with typical layered structure shown in Fig. 1.13, are strongly correlated. As a result one observes many unusual properties, non-Fermi-liquid behavior, a rich phase diagram and antiferromagnetism. Superconductivity depends sensitively on hole doping in the CuO_2 -planes, see Fig. 1.13 for illustra-

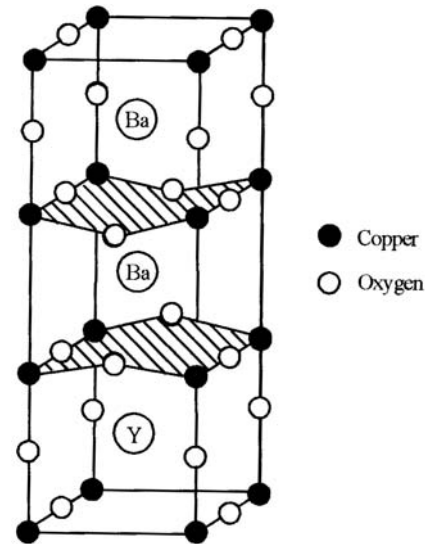


Fig. 1.13. Structure of the cuprate $\text{YBa}_2\text{Cu}_3\text{O}_{7-\delta}$ with T_c up to 92 K depending on hole doping δ . Singlet Cooper pairing occurs essentially in the CuO_2 -planes like in the other members of the cuprate family

tion [22]. It was important that experiments indicated singlet Cooper pairing and d -wave symmetry, see phase-sensitive measurements by Tsuei and Kirtley [23]. Type II superconductivity and non-symmetry of the order parameter, $d_{x^2-y^2}$ -symmetry, is observed. Tunnel spectroscopy, ARPES, and many other experiments support this. Parallel activity (antiferromagnetic and superconducting) occurs. Typically an interdependence of these activities is observed. Singlet Cooper pairing is present. Due to strong correlations unusual properties are exhibited, see, for example, the temperature dependence of the electrical resistivity ($\rho \propto T$) and other transport properties, a pseudo gap of $d_{x^2-y^2}$ -symmetry in the quasi-particle dispersions for lower doping, non-Fermi-liquid behavior (self-energy $\Sigma(\omega) \propto \omega$, etc.), and so on. As a consequence, the elementary excitations in the cuprates seem to behave anomalously. The doping dependence of T_c indicates that phase fluctuations of Cooper pairs play a role, in particular in underdoped cuprates with stronger correlations among the quasi-particles. This seems reflected by

$$T_c \propto n_s, \quad (1.7)$$

where n_s denotes the doping dependent superfluid density ($n_s = n_s(x, T)$). Whether $T_c \propto n_s$ also occurs for electron doping needs to be verified. It is expected for low Cooper pair density.

Figure 1.14 illustrates the doping-dependent phase diagram of hole doped ($\text{La}_{2-x}\text{Sr}_x\text{CuO}_4$)- and electron ($\text{Nd}_{2-x}\text{Ce}_x\text{CuO}_4$)-doped cuprates. In hole doped cuprates for increasing doping x one gets that T_c increases first due to increase of hole concentration and itinerancy and then T_c decreases again due to the disappearance of the antiferromagnetic spin-excitations. Note that electron doping consists largely of occupying the hybridized d -orbitals (upper Hubbard-band) of Cu, of quenching the Cu-spins, while hole doping of the oxygen p -states, destroying long-range antiferromagnetism due to frustration, consists mainly of emptying the oxygen p -band. Thus with increasing hole doping antiferromagnetic excitations are weakened and itinerancy of the correlating hole-carriers is improved. One might expect somewhat different behaviour of hole and electron doped cuprates. Note too that due to correlations

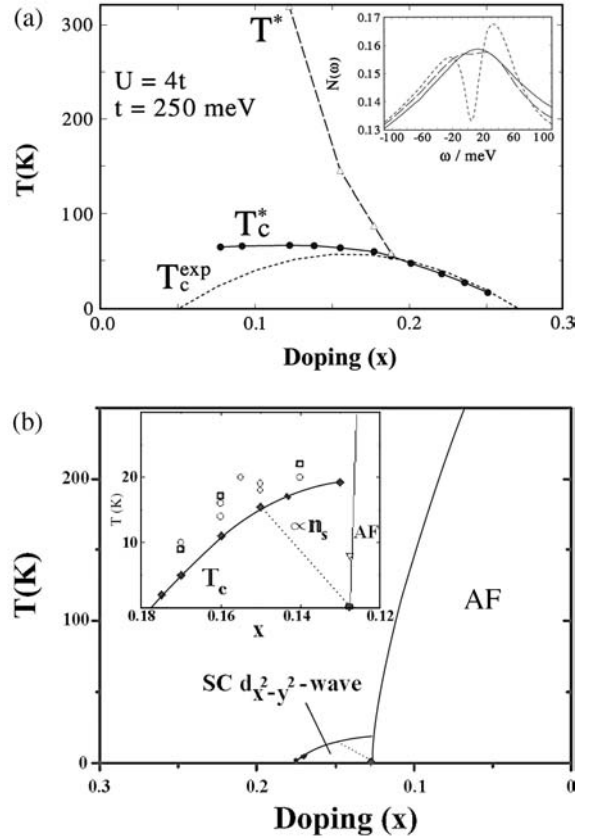


Fig. 1.14. Doping dependence of the superconducting transition temperature $T_c(x)$ of (a) hole ($\text{La}_{2-x}\text{Sr}_x\text{CuO}_4$, ...) and (b) electron ($\text{Nd}_{2-x}\text{Ce}_x\text{CuO}_4$, ...) doped cuprates. T_c^* neglects C.P. phase fluctuations, T^* refers to the onset of pseudo-gap. A.F. refers to the anti-ferromagnetic phase and n_s to superfluid density. The inset in (a) is a calculated spectral density. Note the asymmetry in the spectral density. In (b) the inset refers to calculations of T_c . Here, $T_c \propto n_s$, see the dashed curve, for electron doping is an open question at present

one gets asymmetric peaks in the spectral density. This asymmetry increases for decreasing hole doping. Hence, it is more difficult to add an electron than to extract one in accordance with photoemission experiments. For increasing pd -hybridization this electron-hole asymmetry is expected to decrease.

Typical behavior of cuprate superconductors in a magnetic field reflecting the stiffness of the superconducting wave-function $\psi(\mathbf{r}, t)$ is shown in

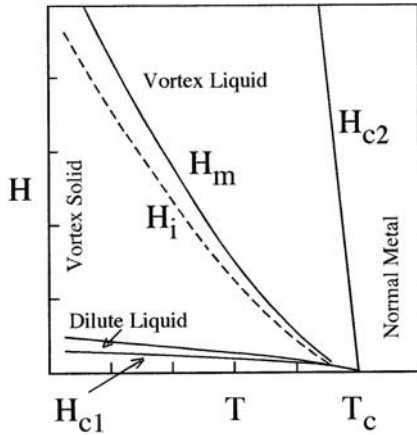


Fig. 1.15. The critical magnetic fields in high T_c -superconductors. Note the steep slope of H_{c2} near T_c . Various phases with vortices occur. Above H_m the melting of the vortex system occurs. H_i refers to the irreversibility field, below which vortices are pinned

Fig. 1.15. New phases of the vortex state were observed. The behaviour in underdoped cuprates is particularly interesting, since the vortex formation is related to the Cooper pair phase ϕ and its stiffness, $\psi(\mathbf{r}, t) = |\psi(\mathbf{r}, t)| e^{i\phi(\mathbf{r}, t)}$. For decreasing doping x the density of Cooper pairs, n_s , decreases and thus phase disorder of the Cooper pairs is expected to play an important role.

The debate on the Cooper pairing mechanism is still under way [24]. Theories mainly by Pines et al. [25], Emery et al. [26], Tewordt et al. [27], Bennemann et al. [28] and others attempt to explain many properties and in particular d -wave superconductivity as resulting from the coupling of the holes in the CuO_2 -planes to antiferromagnetic spin fluctuations. In Fig. 1.16 an Eliashberg-type pairing theory is indicated. In agreement with many experiments one gets for the order parameter $\phi(\mathbf{k}, \omega)$ the results shown in Fig. 1.17. Furthermore, as expected on general grounds one gets also for the electron-doped cuprates like $\text{Nd}_{2-x}\text{Ce}_x\text{CuO}_4$ a d -wave symmetry [29]. For results see Fig. 1.17, and experiments in particular by Kirtley and Tsuei [23].

Note, after the discovery of high T_c superconductors the theoretical developments based on hole-spin-fluctuation coupling were initiated by Scalapino, Bickers [29, 30], Schmalian et al. [31],

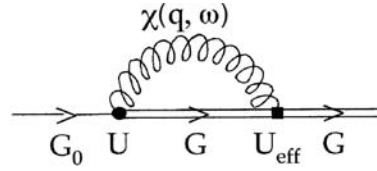


Fig. 1.16. Cooper pairing in the cuprates due to coupling of carriers (holes or electrons) in Cu-O planes to a.f. spin fluctuations characterized by the spin susceptibility $\chi(\mathbf{q}, \omega)$ (G refers to matrix Green's function of quasi-particles, U_{eff} is the effective coupling)

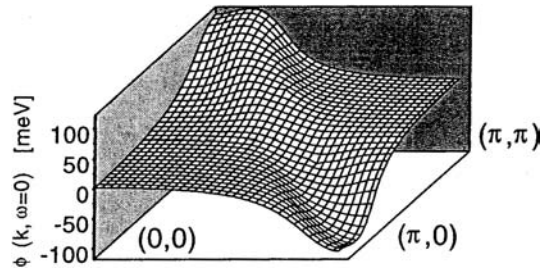


Fig. 1.17. d -symmetry order-parameter $\phi(\mathbf{k}, \omega)$ for hole doped cuprates. In accordance with the CuO_2 -planes we refer to the 2D Brillouin zone with k_x and k_y

and others extending the study by Berk, Schrieffer [20]. Important results were first achieved when careful numerical results were obtained from a self-consistent solution of the spin-fluctuation-type Eliashberg-theory (see Fig. 1.16) [31].

The interesting d -wave symmetry of the superconducting order parameter $\Delta(\mathbf{r}, t)$ or the renormalized one $\phi(\mathbf{k}, \omega)$ can be most simply understood from the general linearized gap function with pairing potential $V_{\mathbf{k}, \mathbf{k}'}$:

$$\Delta_{\mathbf{k}} \simeq - \sum_{\mathbf{k}'} V_{\mathbf{k}, \mathbf{k}'} \frac{\Delta_{\mathbf{k}'}}{2E_{\mathbf{k}'}} \left(E_{\mathbf{k}} = \sqrt{\epsilon_{\mathbf{k}}^2 + \Delta_{\mathbf{k}}^2} \right), \quad (1.8)$$

Clearly, for $V_{\mathbf{k}, \mathbf{k}'} < 0$ (attractive) one may get for constant potential V a \mathbf{k} -independent s -symmetry superconductivity. However, for $V_{\mathbf{k}, \mathbf{k}'} > 0$ (repulsive, as expected for the cuprates due to the strong correlations and occurrence of antiferromagnetism) one gets superconductivity, i.e. solutions of Eq. (1.8), only for \mathbf{k} -dependent pairing $V_{\mathbf{k}, \mathbf{k}'}$ and $\Delta(\mathbf{k})$. In the case of

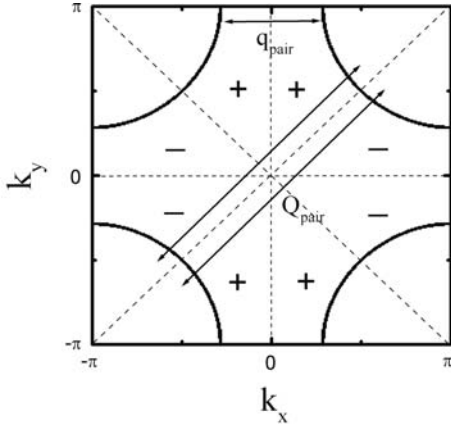


Fig. 1.18. Illustration of *d*-wave symmetry Cooper pairing due to exchange of antiferromagnetic spin fluctuation with wave vector \mathbf{Q}_{pair} between two quasi-particles at opposite parts of the Fermi surface. A quarter of the first Brillouin zone is shown and the signs + and - refer to areas where $\Delta_{\mathbf{k}}$ is positive or negative and a node $\Delta_{\mathbf{k}} = 0$ is indicated by *dashed* lines. If pairing occurs also due to exchange of phonons, for example with wave vector \mathbf{q}_{pair} , then deviations of *d*-symmetry are expected

$V_{\mathbf{k},\mathbf{k}'} \simeq V_{\mathbf{k}-\mathbf{k}'} > 0$ and $\mathbf{k}-\mathbf{k}' \approx \mathbf{Q}$, \mathbf{Q} being the antiferromagnetic wave vector at which the spin susceptibility $\chi(\mathbf{q}, \omega)$ is maximal, one then gets from the combination of the Fermi-surface topology in the cuprates and $\chi(\mathbf{q}, \omega)$ an order parameter of mainly *d*-wave symmetry ($\Delta_{\mathbf{k}} = \frac{\Delta_0}{2} [\cos(k_x) - \cos(k_y)]$). Note that

$\chi(\mathbf{q}, \omega)$ controls the transitions across the Fermi-surface. Note that $V = V\{\chi\}$.

The behaviour of $\Delta(\mathbf{k})$ is illustrated in Fig. 1.17 [32]. If pairing mainly occurs due to exchange of antiferromagnetic spin fluctuations with wave vector \mathbf{Q} , then one expects this to be the strongest for directions in the Brillouin Zone (BZ) where \mathbf{Q} can bridge corresponding portions of the Fermi surface. This is more the case for $(0, \pi)$ than (π, π) directions. Then, the $d_{x^2-y^2}$ -wave symmetry is expected with nodes for the superconducting order parameter along the diagonals of the BZ, see Fig. 1.18 for an illustration. Obviously, Fermi-surface topology (nesting) plays an important role. In view of the Fermi-surface topology and scattering largely by \mathbf{Q} one expects for underdoped cuprates that the spectral density of the quasi-particles is broadest for \mathbf{Q} along $(0, \pi)$ than nodal direction (π, π) . However, for increasing doping and overdoped cuprates \mathbf{Q} does not bridge any more the Fermi-surface along $(0, \pi)$ and thus the spectral-density gets narrower and broadens for \mathbf{Q} -directions (π, π) .

One expects in agreement with experiment significant feedback effects of superconductivity on the dynamical spin susceptibility, $\chi(\mathbf{q}, \omega)$, see inelastic neutron scattering experiments, and on the elementary excitations, see optical conductivity measurements. This interesting interdependence of spin excitations and superconductivity in the cuprates is clearly seen by the change of the dynamical spin

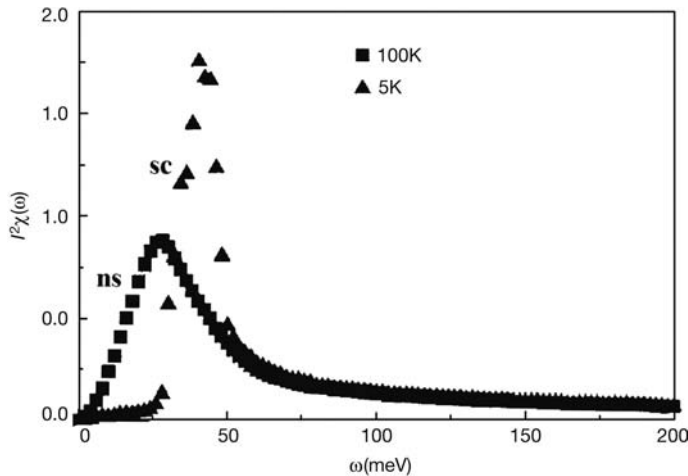


Fig. 1.19. Spin excitation spectrum $\chi(\mathbf{q} = \mathbf{Q}, \omega)$ versus frequency as observed by inelastic neutron scattering (INS) experiments in cuprates [33]. Note the feedback of superconductivity for the spin susceptibility and formation of a so-called “resonance” peak

susceptibility as observed in inelastic neutron scattering experiments (INS), see Fig. 1.19 for results. Of course, this feedback of superconductivity on the spin-susceptibility depends on the topology of the Fermi-surface, distortions, number of CuO_2 -layers per unit cell, doping, etc. Details may serve as a fingerprint of the pairing mechanism. [33]

In Fig. 1.20 results are shown for Δ in electron doped superconductors like $\text{Nd}_{2-x}\text{Ce}_x\text{CuO}_4$. Due to different dispersions $\epsilon_{\mathbf{k}}$ and Fermi-surface nesting one gets a lower $T_c(x)$ than in the hole-doped cuprates. Again, in electron-doped cuprates one also has a d -wave symmetry order parameter, as has been found by Tsuei and Kirtley [34]. Assuming pairing due to an exchange of antiferromagnetic spin excitations this is, of course, expected as shown in Fig. 1.20. Further experiments are necessary to learn about possible different behavior of the electron-doped and hole-doped cuprates. Since in general electron-phonon coupling may also cause superconductivity, this should possibly be taken into account in particular when T_c is smaller. Note that phonon-driven superconductivity yields an s -wave symmetry order parameter. Hence, it might be possible that superconducting transitions due to spin excitations and phonons act together and compete with each other.

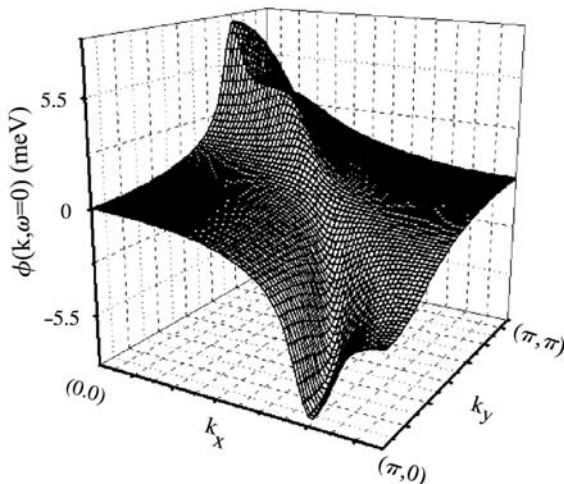


Fig. 1.20. Superconductivity in electron-doped cuprates (such as $\text{Nd}_{2-x}\text{Ce}_x\text{CuO}_4$): Symmetry of order-parameter in the Brillouin zone (doping $x = 0.15$, $T/T_c = 0.8$) [32]. The phase diagram for $T_c(x)$ is shown in Fig. 1.14

(b) Ruthenates

One may say that the study of the high T_c superconductors (exhibiting many interesting features like stripe-structures) during the last 15 years largely occupied the research activity and amusingly enough this might have helped the preparation of new surprises like the triplet Cooper pairing occurring likely in Sr_2RuO_4 , UPT_3 and possibly other systems, i.e. superconductivity in organic materials, and also of the new singlet high T_c superconductor MgB_2 with $T_c \simeq 39$ K. Due to advances in crystal growth the ruthenates have become a very interesting material class in condensed matter physics [35–38]. There are structural similarities with the cuprates [39, 40]. In Sr_2RuO_4 layers of RuO_2 are separated by Sr and O atoms, in SrRuO_3 one has RuO_2 -layers with Sr in between, and in $\text{Sr}_3\text{Ru}_2\text{O}_7$ a similar, but a more 3D-type structure is present. Sr_2RuO_4 is a novel superconductor with $T_c = 1.5$ K observed in 1994 by Maeno [36, 37]. Several measurements indicate triplet Cooper pairing, see the experimental results (NMR-Knight-Shift) shown in Fig. 1.21. Spin triplet Cooper pairing with orbital angular momentum $l = 1$ yields for the order parameter

$$\psi(\mathbf{k}) = a |\uparrow\uparrow\rangle + b |\downarrow\downarrow\rangle + c |\uparrow\downarrow + \downarrow\uparrow\rangle.$$

It seems that in Sr_2RuO_4 due to spin-orbit coupling only the last spin state with zero spin (along the z -direction (perpendicular to the RuO_2 -planes) is in-

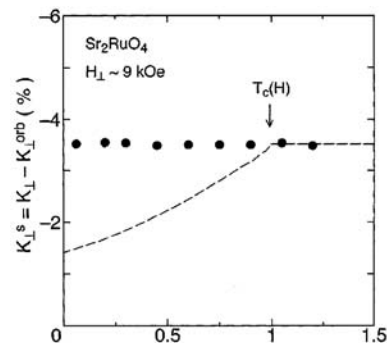


Fig. 1.21. Results for the uniform spin susceptibility in the superconducting state of ruthenates as measured by NMR Knight shift [35]. This seems to demonstrate that Sr_2RuO_4 is a triplet superconductor. Note that the dotted line would occur in case of singlet Cooper pairing (K-Knight shift)

volved. In the presence of a magnetic field also the states $|\uparrow\uparrow\rangle$ and $|\downarrow\downarrow\rangle$ may play a role. In Sr_2RuO_4 one observes a likely p -symmetry for Δ :

$$\Delta_{\mathbf{k}} \propto \mathbf{z} (k_x + ik_y). \quad (1.9)$$

In Fig. 1.22 illustrates results showing the magnetic anisotropy (due to spin-orbit coupling and lattice structure). As a consequence, the anisotropy of H_{c2} is even larger than in the cuprates. SrRuO_3 is a ferromagnetic metal. Upon applying a magnetic field one observes a magnetic quantum critical point in $\text{Sr}_3\text{Ru}_2\text{O}_7$. The Fermi surface of Sr_2RuO_4 is illustrated in Fig. 1.23.

These facts already suggest that the ruthenates are a most important class of new materials in condensed matter physics. In particular triplet Cooper pairs ($\mathbf{k} \uparrow, -\mathbf{k} \uparrow$) in Sr_2RuO_4 may stimulate further studies of triplet pairing in superconducting heavy-fermion metals, in organic systems and ferromagnetic metals like Fe under pressure and a unifying view on superconductivity and ^3He -superfluidity.

Note that superconductivity in Sr_2RuO_4 seems related to both antiferromagnetic and ferromagnetic activity. The superconducting order parameter seems to be of p -symmetry [38,40]:

$$\Delta_{\mathbf{k}} = \Delta_0 \mathbf{z} \cos \frac{k_z c}{2} \left\{ \sin \frac{k_x a}{2} \cos \frac{k_y a}{2} + i \sin \frac{k_y a}{2} \cos \frac{k_x a}{2} \right\}, \quad (1.10)$$

with no nodes in the RuO_2 -planes, but with nodes along the z -direction perpendicular to the planes. The possible form of $\Delta_{\mathbf{k}}$ is illustrated in Fig. 1.24. Note that the spin of the Cooper pairs is parallel to the RuO_2 -planes, but with no preferable direction in these planes. The orbital angular momentum \mathbf{l} of the Cooper pairs points in the z -direction perpendicular to the planes [38,40–42].

Of course, triplet Cooper pairing (breaking time reversal symmetry) is reflected by corresponding thermodynamical and optical behavior. Due to the usual coupling between the orbital angular momentum \mathbf{l} and the external magnetic field \mathbf{h} one expects a rich response and different critical magnetic fields ($H_{c2}(T)$) depending on whether \mathbf{h} is parallel to the RuO_2 -planes or $\mathbf{h} \parallel \mathbf{z}$ perpendicular to the RuO_2 -

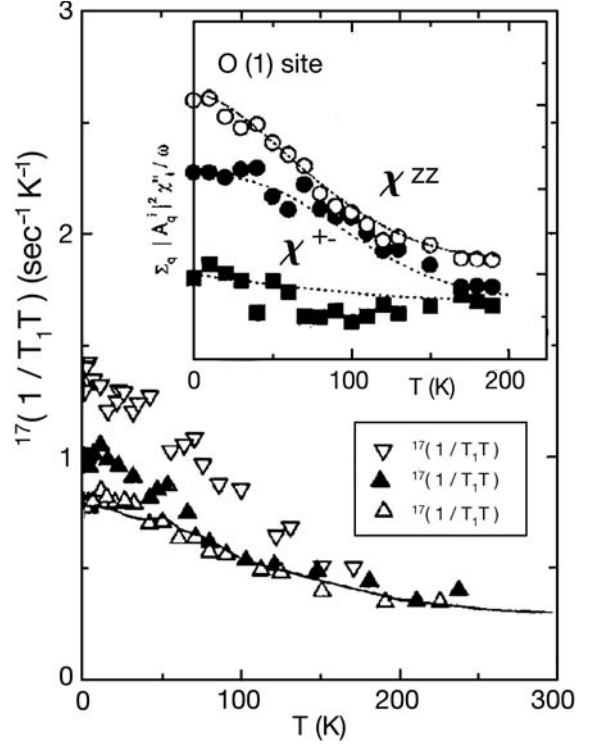


Fig. 1.22. Magnetic anisotropy $\chi^{+-}(T)$ and $\chi^{zz}(T)$ referring to in plane and perpendicular to RuO_2 -plane response, respectively, in Sr_2RuO_4 . The experimental results refer to spin relaxation (T_1 , Knight-shift)

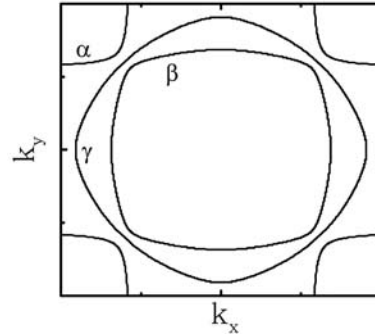


Fig. 1.23. 2D-Fermi surface topology of Sr_2RuO_4 and RuO_2 -planes. α , β and γ denote the FS of the corresponding hybridized bands

planes. Furthermore, the breaking of time reversal symmetry will be seen by corresponding optical response, for example, its dependence on light polar-

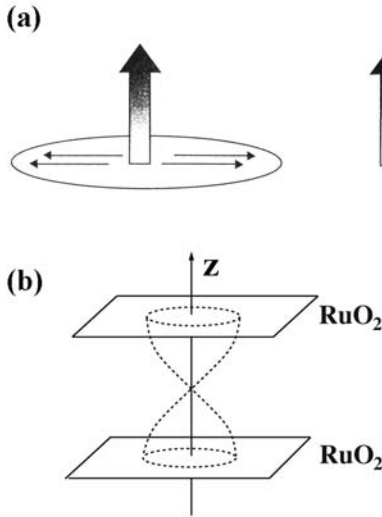


Fig. 1.24. Illustration of a possible form of the p -type superconducting order parameter in Sr_2RuO_4 . (a) Spin triplet states in superconducting Sr_2RuO_4 corresponding to $\Delta \sim z(k_x + ik_y)$, with angular momentum parallel to z -axis and spins perpendicular, and $\Delta \sim xk_x + yk_y$, with vanishing angular momentum. Clearly, an external magnetic field and spin-orbit coupling will control the most stable triplet state. (b) Illustration of the amplitude of the order parameter. In principle incommensurability along the z -axis may occur

ization. The magnetic anisotropy is expected to lift the degeneracy of the three triplet states ($|\uparrow\uparrow\rangle$, $|\downarrow\downarrow\rangle$, $|\uparrow\downarrow\rangle + |\downarrow\uparrow\rangle$) [40].

Note that it is of utmost significance to identify definitely triplet pairing and the pairing field (spin-excitations).

c) Heavy-Fermion Metals

The heavy-fermion metals like CeIn_3 , UPt_3 , etc., are characterized by an unusually large electronic density of states (DOS) near the Fermi energy, $N(0)$. Thus, the effective mass m of the carriers is much larger than the bare electronic mass m_0 . Note, m may range up to $100 m_0$ or more. Typical heavy-fermion metals are listed in Table 1.1 [42–45].

Table 1.1. List of heavy-fermion metals. m and m_0 are the effective and bare electron mass and T_c the superconducting transition temperature. Note the interesting dependence of T_c on pressure

	UPt ₃	UPt ₃	UPd ₂ Al ₃	UGe ₂
m/m_0	360	1100	210	100
$T_c(\text{K})$	0.55	0.85	2	0.7

Due to the large electronic density of states (DOS) the heavy-fermion metals exhibit simultaneously interesting magnetic and superconducting behaviour. Multiple magnetic and superconducting phases and generally complex thermodynamical behaviour exist [45,46]. For example, this is demonstrated by the phase diagrams of $T_c(h)$ and $T_c(P)$ of UPt_3 shown in Fig. 1.25.

Note, while in conventional type II superconductors there are two superconducting phases in the h - T plane (a low field Meissner phase and a high field vortex phase above $h_{c1}(T)$); in UPt_3 there are five phases: vortex phase C, and phases A and B each exhibiting a Meissner and vortex phase. The phase diagram $T_c(P)$ also exhibits the superconducting phase A, appearing for pressure $P=0$ at $T_c \geq 5$ K, and phase B appearing

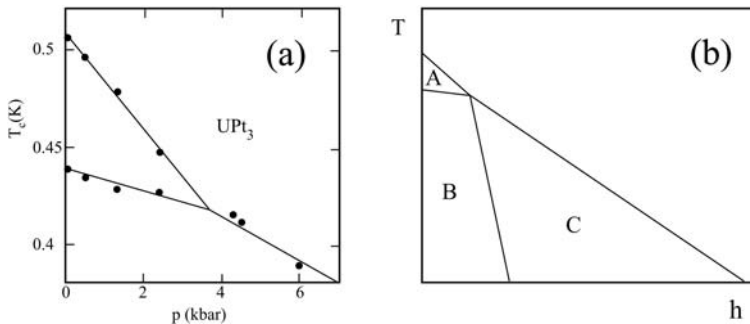


Fig. 1.25. The phase diagram (a) $T_c(P)$ and (b) $T_c(h)$ of the heavy-fermion metal UPt_3 is shown (h denotes the external magnetic field, p the pressure). A, B, C refers to different superconducting states

for $P=0$ at $T_c \simeq 0.44$ K. The symmetry of the order parameter is certainly not simply s -wave like, but different for $T_c(P, h)$. This is still being analyzed as well as the mechanism for Cooper pairing. However, spin-excitations are probably involved.

Several studies have been performed for analyzing the superconducting phases by using a Ginzburg–Landau theory and allowing a more complex order parameter including triplet Cooper pairing. Note that the free-energy change may be described by

$$\Delta F = \alpha_1(T - T_{c1})|\Delta_1|^2 + \alpha_2(T - T_{c2})|\Delta_2|^2 + \beta_1|\Delta_1|^4 + \beta_2|\Delta_2|^4 + \beta_{12}|\Delta_1|^2|\Delta_2|^2 + \dots \quad (1.11)$$

Here, Δ_1, Δ_2 refer to the order parameter of the different phase transitions. The coefficients are pressure dependent. Then in the usual way one attempts to derive the observed phase diagrams from Eq. 1.11.

In Fig. 1.26 we show more data on heavy-fermion metals indicating the role played by magnetic excitations. The superconducting transition-temperature $T_c(p)$ of CeIn_3 may be of particular interest due to quantum criticality at $p \simeq 28$ kbar where the Néel temperature decreases ($T_N \rightarrow 0$) and superconductivity

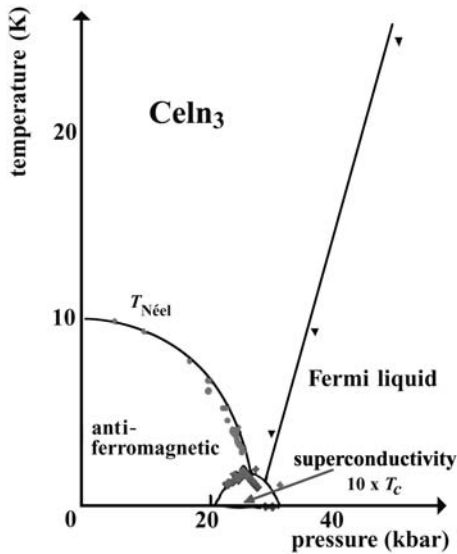


Fig. 1.26. Phase diagram of the heavy-fermion CeIn_3 . Note the appearance of superconductivity at larger pressure. A quantum critical point occurs at about 28 kbar

appears [46]. This, however, needs further studies. Note the interplay of a.f. and superconductivity and the changes due to pressure (itineracy of carriers is expected to increase with pressure). As in CePd_2Sr_2 and other heavy-fermions a quantum critical point seems present. An interesting phase diagram is also observed for UGe_2 with an interplay of ferromagnetism and superconductivity. Here a ferromagnetic quantum critical point possibly plays a role. The behaviour of Fe under pressure effects in particular the important interplay of structure, ferromagnetism and superconductivity. The origin of superconductivity needs to be studied.

It is of utmost interest to determine for UPt_3 and the other heavy-fermion, for Fe and UGe_2 , see Fig. 1.27, and related metals the interplay of mag-

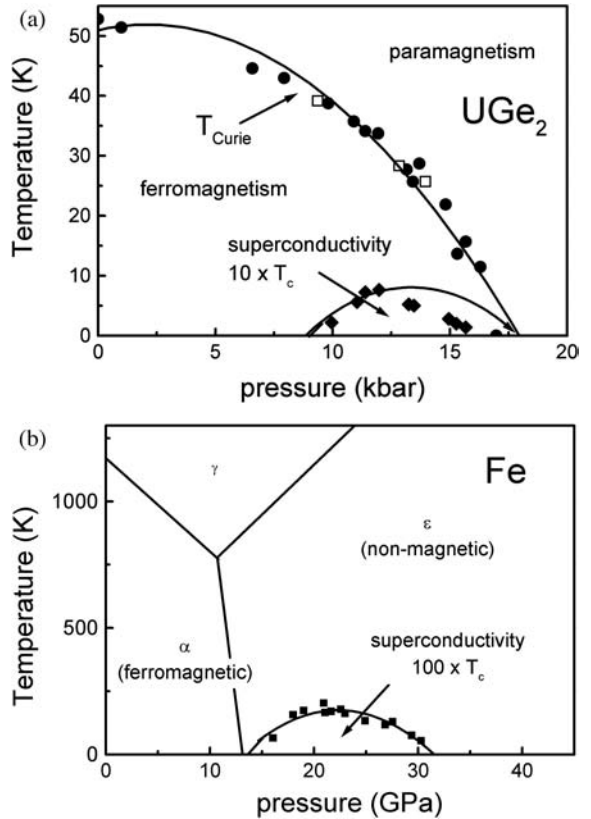


Fig. 1.27. (a) Phase diagram of UGe_2 . (b) Superconducting hexagonal ϵ -phase Fe under strong pressure. α, γ, ϵ refers to the various Fe phases (α : bcc, ϵ : hcp)

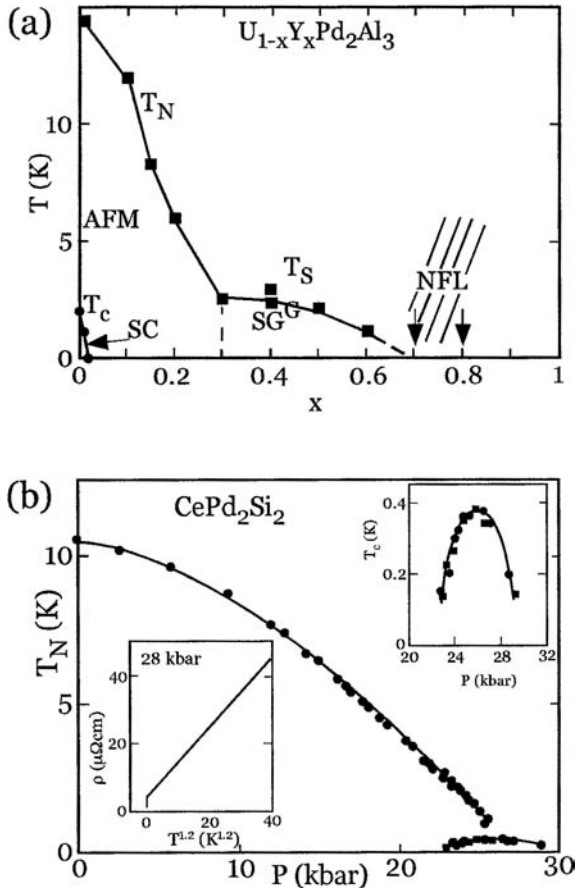


Fig. 1.28. Superconductivity in heavy-fermion systems: (a) Typical complex phase diagram, (b) pressure induced superconductivity. (Here, T_N refers to the Néel temperature, T_{SG} to the spin-glass temperature, NFL to nearly Fermi-liquid behavior, and ρ to the electrical resistivity)

netism and superconductivity, the symmetry of the superconducting order parameter, the thermodynamical properties and the role played by quantum critical points (Q.C.P.). Besides Ginzburg–Landau type analysis electronic theories are needed to understand superconductivity in these systems.

To summarize, the interdependence of magnetism and superconductivity has been a classical problem and nowadays seems to have regained interest due to technical advances. Note that the Larkin–Ovchinnikov state of a superconductor in the presence of an exchange field [47]

$$\Delta_k \sim \cos(\mathbf{k} \cdot \mathbf{r}) \quad (1.12)$$

also indicates that magnetism and superconductivity may seek a compromising arrangement. This is also known from Ginzburg–Landau theory with two order parameters, which may coexist or exclude each other, depending on the parameters controlling the energetics.

Further interesting phase diagrams are shown in Fig. 1.28. Not much is known about the pairing mechanism and symmetry of the superconducting state appearing upon alloying and applying pressure. Such typical phase diagrams are again indicative of the interplay of structure, antiferromagnetism or ferromagnetism and Cooper pairing. Note that further experiments may somewhat modify these interesting phase diagrams and offer new insight.

Organic Superconductors

Recently, many studies have shown that organic metals are most interesting. A large class of crystalline organic systems are quasi-two-dimensional charge-transfer salts. Many become superconducting [48]. Various properties of these organic metals are shared with the cuprates, such as layered structures, strong correlations causing also antiferromagnetism and non-s-symmetry Cooper pairing. The organic metals are very clean, nearly impurity free systems. Moreover, astonishingly, superconductivity may be induced by strong magnetic fields.

In Fig. 1.29 the interesting phase diagram of κ -(BEDT-TTF) $_2$ -Cu[N(CN) $_2$]Br, a typical composition of a charge-transfer salt, is shown. Such molecules are stacked into layers. Planes of Cu[N(CN) $_2$]Br anions separate these layers. Within these layers the molecules form dimers and electrons or holes can then hop easily from one molecule to the next, but not perpendicular to the layers (hence: quasi 2D-behavior). Thus, salts consist of conducting layers separated by a non-conducting environment (anions).

Clearly, bond-length changes, also due to pressure, will sensitively change the electrical properties. Also applying a magnetic field perpendicular to the layers (along the c -axis) affects the system due to the formation of Landau-levels that will pass the Fermi

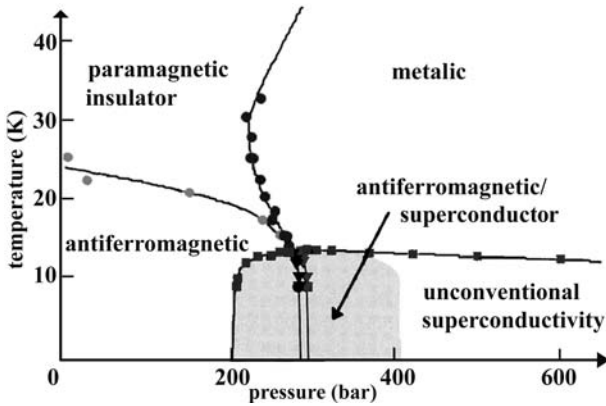


Fig. 1.29. Phase diagram of the organic metal κ -(BEDT-TTF)₂-Cu[N(CN)₂]Br (Bisethylenedithio-terathiofulene-X type salt) from N.M.R. and A.C. susceptibility

energy as the external magnetic field varies (see de Haas-van Alphen oscillations). In stronger magnetic fields quantum mechanical interband tunneling also occurs, see Singleton et al. [48].

Superconductivity occurs at relatively low temperatures usually upon applying pressure, see Fig. 1.29. Various experiments indicate unconventional Cooper pairing ($2\Delta_0 \sim 7k_B T_c$, non-s-symmetry of Δ_k). Note superconductivity occurs close to the antiferromagnetic-state like in the cuprates and heavy-fermion metals. Experiments indicate that the long range magnetic order is due to localized spins on the dimer and not due to the hopping carriers (holes or electrons). Antiferromagnetic spin-fluctuations occur as a precursor of superconductivity. How much these and phonons are involved in Cooper pairing must be clarified by further analysis. Theoretical studies are presented by Schmalian and others.

In an external magnetic field interesting behaviour may result due to the layered structure, Landau-level formation and spin-split bands. Possibly Cooper pairs ($\mathbf{k} \uparrow, -\mathbf{k}+\mathbf{q} \downarrow$) may form. A Larkin-Ovchinnikov state [47, 48] with $\Delta_k \sim \cos(\mathbf{k}\mathbf{r})$ may occur. In general, the response to an external magnetic field is highly anisotropic. Furthermore, it is interesting that superconductivity may be induced in λ -(BETS)₂FeCl₄ by a magnetic field h , which destroys long range magnetic order of the Fe³⁺. Field induced superconductivity may also occur in α -(BEDT-TTF)₂KHg(SCN)₄ by affecting with the external magnetic field h the charge-density-wave (CDW) present in this system.

Clearly further experiments are needed to clarify the situation. However, rich behaviour may be expected in general, since CDW, SDW excitations, Landau levels and 2D properties are present. The different excitations and phases may cause inhomogeneities (as a compromise to gain maximal energy).

1.3 Granular Superconductors, Mesoscopic Systems, Josephson Junctions

As early studies by Buckel and Hielsch and others have shown strongly disordered lattices and amorphous metals may affect superconductivity due to changes in the electron-phonon coupling, the phonon-spectrum, the electronic parameters (DOS:N(0)) and surface effects. As a result superconductivity changes and might be strengthened, there is an increase of T_c , and generally thermodynamical properties might change favorably, see Garland, Bennemann [49], and Deutscher and references therein. In the amorphous state some non-metallic systems become metallic and then also superconducting. In Table 1.2 we illustrate the situation.

Remarkable is also the occurrence of superconductivity in PdH-systems where dramatic changes in T_c (that are dependent on H-doping and disorder) are observed, see experiments by Buckel et al. [49, 50].

This is a good example of the potential of material science regarding superconductivity studies. Similarly this is the case for superconductivity in fullerenes.

Table 1.2. Superconductivity in disordered and amorphous metals. Estimates of the superconducting transition-temperature T_c by Bennemann et al. [49] (T_{c0} refers to the crystalline structure)

material	$(T_c/T_{c0})_{expt}$	$(T_c/T_{c0})_{calc.}$
Al	~ 5	4.9
Pb	~ 0	0
Ga	~ 8	8
Sn	~ 1.3	2
In	~ 1.3	1.2

Extending these studies of granular materials, small particles, nanostructures and metals consisting of an ensemble of small metallic grains and clusters have been investigated [51], see Fig. 1.30. Thus, quantum size effects occur (discretization of electronic energy spectrum: $\epsilon_k \rightarrow \epsilon_n$, granular size $l \sim \xi$, λ ; ξ is the coherence length and λ the penetration depth).

In such granular superconductors surface effects and proximity effects become important. As a function of grain size metal insulator transitions and strong quantum-mechanical behaviour occurs. Note that on general grounds one expects, for example, that in reduced dimensions fluctuations play a more important role. (Also, different Cooper pairing mechanisms and singlet and triplet pairing are expected to depend differently on particle size.)

The discretization of the electronic energy spectrum, $\epsilon_k \rightarrow \epsilon_n$, is illustrated in Fig. 1.31. Of course, the level spacing $\delta(T)$ affects various properties such as the coherence-length $\xi(n)$ and penetration depth $\lambda(n)$ and thus the thermodynamical and optical properties. Note that $\xi/R \sim N^{2/3}$ and hence $\xi \gg R$ due to $N^{2/3} \gg 1$. One expects that superconductivity disappears below a critical particle size ($R < \xi$). The behaviour of small particles due to changes in the number n of electrons, for example $n \rightarrow n \pm 1$, and Cooper pairs by 1, for example, is very interesting and may play a role in achieving a two-level superconducting state (two charged states). This may possibly be used for information technology (information storage, optical imprinting technology).

The charging of small particles is controlled by the electrostatic energy. The change of the charge

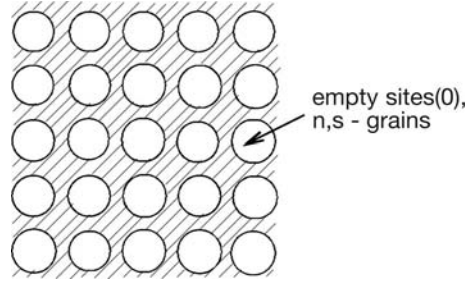


Fig. 1.30. Illustration of an ensemble of small particles, grains which are in the normal (n) or superconducting (s) state. For small particle size (radius R) and volume V the electronic energy spectrum gets discrete with level spacing $\delta(\delta = (N(0)V)^{-1} \approx \epsilon_F/n = (\hbar V_F/R)(Rk_F)^{-2}$; $N(0) = \text{DOS}$ at ϵ_F , $n = \text{no of electrons}$). The grains may be in the normal (n) or superconducting (s) state. In such a grain structure some sites may be empty (0). Note, such a lattice-like structure may resemble an alloy of s and n state grains and also a nanostructure if small particles are removed irregularly from the lattice (empty sites)

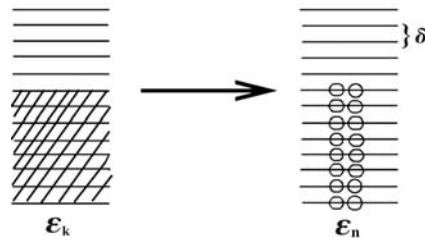


Fig. 1.31. Illustration of size effects in small particles having a diameter of the order of R and n -electrons. The level spacing is $\delta \approx \epsilon_F/n \approx (\hbar V_F/R)(k_F R)^{-2}$ and the coherence length $\xi \sim (R\delta/kT_c)(Rk_F)^2 = \delta_0 N^{2/3} R$. Here, we introduced the dimensionless size parameter $\delta_0 = \delta/kT_c$

$Q = en \rightarrow Q \pm 1$ causes an energy change $e^2/2C$; C is the capacitance of the small particle and this may lead to a Coulomb blockade (in tunneling, for example). Approximately at temperatures $T \simeq 0$ due to the electrostatic energy ($Q = e\Delta n$, $Q' = C'V$ being the charge at the electrodes of the applied voltage) it is

$$E_n = \frac{Q^2}{2C} - \frac{Q}{C} C' V \quad (1.13)$$

(C, C' capacitances, V =external potential). The Coulomb blockade is periodically lifted as a function of n and V when $E_{n+1} = E_n$. In the superconducting

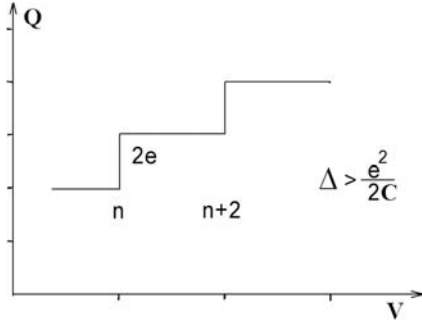


Fig. 1.32. Charging up behavior of a small superconductor with capacitance C and charge $Q = en$, n -even, in a potential ($\Delta > e^2/2C$). This behavior ($2e$ -jumps and $2e$ -periodicity in V) follows from $E_n = E_{n+2}$ and n -even and reflects Cooper pair formation. One has also $E_n = E_{n+1} + \Delta$, where E_{n+1} has one unpaired electron. Then Q changes by $2e$ at corresponding external voltage. Again one has a $2e$ -periodicity in the energy level structure

state for $T \simeq 0$ and $\Delta > e^2/2C$ one has the situation illustrated in Fig. 1.32. From $E_{n+2} = E_n$, n -even and a large Cooper pair sea, one gets a period-doubling with respect to the normal state of the charge periodically of energy levels, of the jumps in Q at voltages V which lift the Coulomb blockade ($V \propto (2n+2)$). Note that $E_{n+2} = E_n$ might not hold for smaller density of Cooper pairs. For E_{n+1} with one unpaired electron at energy Δ above the ground-state one has $E_n = E_{n+1} + \Delta$ to determine the $2e$ charge periodicity. This gives the even-odd number parity, see Tinkham et al. and Nozarov [52]. Charge transfer occurs for the small particle when energy levels cross.

In view of the strong quantum-mechanical behavior of small particles structures consisting of a larger number of small particles seem very interesting (mesoscopic systems). Note that the charging up behavior will reflect spin and thus may be different for singlet and triplet Cooper pairing. Also the behaviour of grains is related to the one of Fermions in optical lattices.

An ensemble of grains may exhibit transitions to superconductivity at T_{c1} , where the single grains are superconducting, and at T_{c2} where globally and phase coherently the whole ensemble becomes superconducting ($T_{c2} \leq T_{c1}$ and $zE_J \geq E_c$); for an illustration see Fig. 1.33. Generally an ensemble of grains may resemble an alloy like array of S/S and

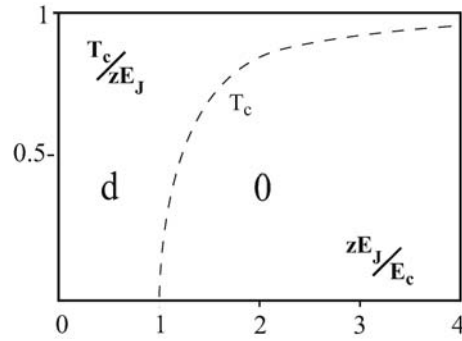


Fig. 1.33. Transitions in an ensemble of superconducting quantum dots controlled by the Josephson energy E_J and the Coulomb energy $E_c = e^2/2C$. T_c refers to the global superconducting transition-temperature of the ensemble. Phase O below T_c refers to a globally ordered superconducting state of the ensemble and phase d above T_c to superconducting grains with no global Cooper pair phase coherence. z is the coordination number

S/N junctions. (S = superconducting, N = normal state grains.)

Of course, the behavior of an ensemble of grains depends on the coupling, i.e. on electron hopping between the grains. The structural order of the grains also plays a role. A regular lattice-like arrangement of the grains (1D, 2D-topology) is of particular interest. For small distances between the cluster particles electron tunneling, inelastic Cooper pair tunneling (Josephson coupling) occurs. Hence, charge fluctuations are present in such granular superconductors. The resultant interesting Josephson effect can be described by [52]

$$H = H_T - \sum_{i,j} E_J(i,j) \cos \Phi_{ij} + \frac{2e^2}{C} \sum_{i,j} (N_i - N_j)^2 + \dots \quad (1.14)$$

In Eq. (1.14) the first term refers to normal electron hopping between the grains, the second term to Cooper pairs tunneling between neighboring superconducting grains (Josephson effect), and the last term is electrostatic energy due to different charges of neighboring grains i, j . For simplicity, the same capacitance C and E_J -Josephson energy is taken. The phase difference $\Phi_{ij} = \Phi_i - \Phi_j$ refers to the phases Φ_i of the superconducting order parameter $\Delta_i = |\Delta_i|e^{i\Phi_i}$ of grain i . It is important to note that

$$[\Phi, N] = i, \quad (1.15)$$

where N is the Cooper pair number operator [51,53]. Hence, Φ and N are canonically conjugate variables. Treating these as classical variables from the Hamilton-Jacobi equations one immediately finds the Josephson equations

$$j_J = (E_J/e) \sin \Delta\Phi \quad (1.16)$$

and

$$\dot{\Phi} = 2eV. \quad (1.17)$$

Note that the commutator Eq. (1.15) implies the uncertainty relation

$$\Delta\Phi\Delta N \sim 1. \quad (1.18)$$

Consequently, large phase fluctuations, i.e. the phase incoherence of the small particles imply a ΔN and thus N is a good quantum number. Hence, in view of Eq. (1.18) in an ensemble of superconducting grains one may expect an ensemble transition to a Mott-insulator if the capacitance C becomes smaller and thus the Josephson energy ($\sim E_J$) becomes smaller than the electrostatic energy $\sim 2e^2/C$ [51,52]. The charge transport between the grains is suppressed while each grain is still superconducting. This behaviour is illustrated in Fig. 1.33 [52].

Note that if the capacitance C becomes larger, ΔN increases and then all grains become phase coherent ($\Delta\Phi \rightarrow 0$) [51,53]. These thoughts apply also to fermions in optical lattices and corresponding phase transitions.

For small particles (of size <10 nm, for example) the proximity effect and the Andreev-reflection [51,54] play an increasingly important role and may cause anomalous behaviour of the diamagnetic susceptibility and of the maximal Josephson currents as a function of particle size, temperature, etc. For example, the Josephson currents ($j_J = j_0 \sin \Delta\Phi$, $j_0 = \pi\Delta/2eR_T$, R_T resistance of tunnel barrier) may reverse ($j_J \rightarrow -j_J$, π -junctions) and the maximal current j_0 reflects quantum size effects. In a Josephson lattice of quantum dots one has $j_0 = z\frac{e\Delta}{\hbar}$, where z is the lattice coordination number [51]. The ensemble topology of the small particles and their separation plays a role, since mean free path effects and phase

coherency matter. A ring-like arrangement of Josephson coupled quantum-dots is expected to be an interesting physics toy regarding behaviour of two-state superconductors and flux-pinning [52].

Tunnel Junctions

It is obvious that tunnel junctions have become an interesting new area of solid state physics [55,56]. The tunnel medium (metals, insulators, molecules) can be manipulated, in particular optically, and new non-equilibrium physics may result. In Fig. 1.34 we illustrate a tunnel junction describing in particular S/N/S, N/S/N junctions. Here, S may refer to singlet or triplet superconductors and N to normal state systems, metals and ferromagnets [54]. In the case of an $S_1/N_2/S_3$ sandwich, where S_1 and S_3 are singlet BCS-type superconductors, the spin tunnel current is zero. If S_1 is a singlet and S_3 a triplet superconductor, one expects for Josephson tunneling [54]

$$j_j = \sum_n (j_{1n} \sin n\Delta\phi + j_{2n} \cos n\Delta\phi).$$

Here, $n = 1, 2, \dots$ and $\Delta\phi$ refers to the phase difference of the order parameter of S_1 and S_3 . We assume that the thickness $2d$ of N_2 does not destroy phase coherence of the tunneling electrons. Equation (1.19) corresponds to a general Fourier-expansion of j_j . If time reversal symmetry is present (both S_1 and S_3

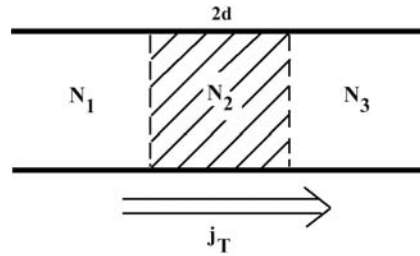


Fig. 1.34. Illustration of a tunnel junction $N_1/N_2/N_3$, where N_i may refer to singlet and triplet superconductors and to normal state metals, including ferromagnets, respectively. The tunnel current j_T may refer to single electrons or Cooper pairs and transport of charge and spin. Depending on the thickness $2d$ of the tunnel medium proximity effect and Andreev-reflection at S/N interfaces plays a role. Note that applying a voltage to the tunnel junction may yield a two-level system with no or one extra Cooper pair on superconductor 3 (qubit)

are singlet B.C.S. superconductors) the second term in Eq. (1.19) disappears, since $\Delta\phi \rightarrow -\Delta\phi$ implies $j_J \rightarrow -j_J$. Then one has approximately $j_J \sim \sin \Delta\phi$. If S_3 , for example, refers to a triplet superconductor, then characteristically

$$j_J(n=1) = 0, \quad (1.19)$$

since the superconducting wave functions $\psi_i = \eta_i^{\text{spin}} \varphi_i^{\text{orbital}}$ of $i=1$ and $i=3$ are orthogonal [54]. Thus to lowest order for a (singlet/ N_2 /triplet) sandwich

$$j_J \sim \sin(2\Delta\phi) + \dots \quad (1.20)$$

Clearly spin-active interfaces of the sandwich resulting from spin-orbit coupling or spin-excitations in N_2 may change the symmetry arguments and then $j_J(n)$. Note, in the case of spin-flip scattering selection rules change and spin and orbital angular momentum need not to be conserved separately, but only the total angular momentum. As a consequence, one might get contributions from j_{11} and j_{21} and from higher j_{in} .

In summary, one expects characteristic properties and differences for the (singlet/ N_2 /singlet), (singlet/ N_2 /triplet), and (triplet/ N_2 /triplet) junctions. Similarly, if N_2 is a ferromagnetic metal or insulator it will affect differently and characteristically junctions involving only singlet superconductors and those involving a triplet superconductor. Clearly, Josephson tunneling of singlet Cooper pairs is more characteristically affected by a ferromagnet N_2 tunneling medium than j_J for triplet superconductors. In particular, recent studies have shown the physical richness of behaviour expected for tunnel currents, see Morr et al. for an illustration [56]. Sandwiches ($F_1/S/F_3$) involving a superconductor S between two ferromagnets F_1 and F_3 with parallel or antiparallel orientation of the magnetization will also exhibit interesting behaviour. (We assume for simplicity that the thickness $2d$ of S is smaller than the spin-mean free path in S .) Then charge (j_c)-tunnel and spin (j_{sp})-tunnel currents are expected. Due to spin-polarized tunnel currents provided by the exchange splitting of majority and minority bands in the ferromagnets one gets, in general, the functional behaviour

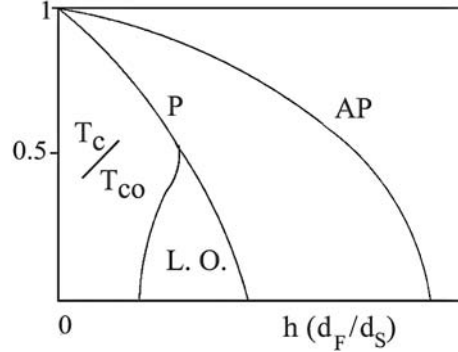


Fig. 1.35. Phase-diagram of an ($F_1/S/F_3$) sandwich. S refers to a singlet superconductor and F_1, F_3 to ferromagnets with T_c at P for parallel (P) orientation of their magnetization and T_c at AP for antiparallel (AP) one. $L.O.$ is the Larkin-Ovchinnikov phase, h the exchange field and T_c and T_{co} the superconducting transition-temperature in the presence and absence, respectively, of the exchange field. d_F and d_S refer to the thickness of the ferromagnetic and superconducting film, respectively

$$j_T = j_T\{\Delta, \dots\}, \quad \Delta = \Delta\{j_T, \dots\}. \quad (1.21)$$

The spin-polarized tunnel current j_T may cause the presence of unpaired single electrons at the Fermi energy ϵ_F besides Cooper pairs, and thus superconductivity is weakened. The effect should be different for singlet and triplet-Cooper pairs. A rich thermodynamical behaviour is expected. Due to the proximity effect and Andreev-reflection [51, 54] the F/S interface coupling may cause the induction of a Larkin-Ovchinnikov state [47] into the singlet superconductor ($\Delta_k \rightarrow \Delta_0 \cos kx + \dots$), for example if $\lambda \sim 2d$. Then the electrons in the superconductor may feel the exchange field present in the ferromagnets. Also the exchange field accompanying the spin-polarized tunnel current might cause a similar change of the Cooper pairing.

For sandwiches ($F_1 | S | F_3$) with a singlet superconductor one gets the results shown in Fig. 1.35. Corresponding results are expected for such a sandwich with a triplet superconductor. Then the phase diagram is determined by the coupling of the Cooper pair spin (angular momentum) to the exchange field \underline{h} . Applying Usadel-type and Eilenberger-type equations [54] for Cooper pairing in external fields \underline{h} one has

$$\left\{ \omega'_n + ih(\mathbf{r}) + \frac{1}{2} \mathbf{v}_F \cdot \nabla \right\} F = \Delta'(\mathbf{r})G,$$

$$\omega'_n = \omega_n + \frac{1}{2\tau} \int \frac{d\Omega}{4\pi} G(\mathbf{r}),$$

and

$$\Delta'(\mathbf{r}) = \Delta(\mathbf{r}) + \frac{1}{2\tau} \int \frac{d\Omega}{4\pi} F(\mathbf{r}). \quad (1.22)$$

Here, G and F are the usual Green's functions and τ is the elastic scattering term. Thus, one obtains the interesting phase diagram for $(F_1/S/F_3)$ sandwiches shown in Fig. 1.35. [54,55]

Recently, Nogueira and Bennemann discussed a Josephson-like spin current j_f^{spin} for $(F_1/N_2/F_3)$ -sandwiches [53]. If the thickness $2d$ is smaller than the spin-mean free path the results could also be applied if N_2 is a superconductor.

1.4 Outlook

In summary, this overview shows that the history of superconductivity has been full of surprises and that superconductivity is a stimulating and continuing problem of physics. A theory like the BCS-theory for phonon-mediated superconductivity would be of utmost significance for the novel superconductors. The pairing mechanism, symmetry of the order parameter and the superfluid density are central issues. More detailed knowledge on the magnetic activity in the cuprates, etc., on local versus itinerant magnetism (see $\chi(\mathbf{q}, \omega)$, etc.), and on short-range spin ordering is needed. Correlations (local repulsion) cause a particle-hole asymmetry reflecting that it is more difficult to add an electron than to remove one and this affects many properties. Future studies may change some parts of our present physical picture, will extend our knowledge, and will certainly bring new discoveries. As was recently demonstrated by Homes [57], the superconducting transition temperature T_c may be scaled for many materials in a unifying way according to

$$\rho_s \sim \sigma_{DC} T_c. \quad (1.23)$$

Here, ρ_s and σ_{DC} refer to the superfluid density at $T=0$ and the electrical conductivity, respectively. This

scaling follows immediately from the general formula $\rho_s = (m/e^2)\omega \text{Im}\sigma(\omega)$. As a special result one gets the Uemura scaling $\rho_s \sim T_c$ for underdoped high T_c -superconductors. Note,

$$\rho_s = (\omega\sigma''/\sigma'_{DC}T_c)_{\omega=0} \cdot \sigma_{DC}T_c = \text{const.}(\sigma_{DC}T_c),$$

if $\sigma_{DC}T$ is independent of temperature.

We have attempted to summarize recent developments in the area of superconductivity. Superconductivity in MgB_2 , cuprates, ruthenates, heavy-fermion metals (material) and organic systems shows that new metals continue to keep the field alive. This view is further supported by the results on small particles, nanostructures and sandwich-structures. The interdependence of structure and superconductivity and further of magnetism and superconductivity remains a key physical issue. In particular tunneling probing sensitively the superconducting state is of interest [56]. In tunnel junctions (SC/FM/SC) the magnetic medium FM may affect (tune) the phase between the superconductors (SC) and cause spin-polarization of the tunnel current and the current may be manipulated by an external magnetic field. Extreme quantum-mechanical behaviour due to $T \rightarrow 0$, reduced dimensionality, correlations, quantum-fluctuations and in particular quantum critical points (QCP) might present new surprises in the future. New non-equilibrium behaviour, optical studies probing the superconducting state and (fast) switching phenomena involving superconductivity will be interesting. Of course, the search for new superconductors still remains interesting. Superconductivity in intercalated systems like $\text{Na}_x\text{CoO}_2(\text{H}_2\text{O})_y$, (for $x \approx 0.35$ and $y \approx 1.3$ $T_c \leq 5\text{K}$ [58]) may serve as an example. In liquid metallic hydrogen (H), obtained upon applying pressure, besides other phases superconductivity may occur [59]. Under pressure hydrogen becomes liquid and exhibits an insulator to metal transition. One gets a ground-state quantum-liquid metal. In the presence of a magnetic field liquid metallic hydrogen (free energy: $\Delta F = \sum_{i=e,p} [|\nabla \pm ie\mathbf{A}\psi_i|^2/2m_i + V(|\psi_i|^2)] + \frac{B^2}{2}$, $B = \nabla \times \mathbf{A}$, i refers to electrons and protons) exhibits several phase transitions with strong quantum mechanical features, superconductivity and superfluidity as was shown by Babaev, Sudbo, Ashcroft et al. [59].

A liquid metal close to the ground state ($T \rightarrow 0$) and ordered quantum mechanical fluids (a superconductor or a superfluid of protons and electrons, two-fluid system) are obtained. In the presence of an external magnetic field several phase transitions to ordered states, between superconductor and superfluid, occur. This may be of general significance, in particular for astrophysics. Note, hydrogen amounts to about 90% of all elements and constitutes due to the light mass and zero-point energy strongly quantum-mechanical systems. Metallic H may become a type II superconductor and under higher pressures electrons and protons form a 2 component Fermi-liquid, Cooper pairs of protons and of electrons form and may coexist. In a magnetic field interesting novel structures of vortices may occur. The pairing potentials needs to be studied by a microscopic theory.

A unifying field theoretical analysis of non-Fermi liquid behaviour and of superfluidity and of Bose-Einstein condensation (BEC) remains a challenging goal. Ultracold Fermi gas may become superfluid and then tuning the interactions (in an optical lattice, for example) one observes a BCS-state, BEC and a crossover transition. As the size of the singlet Cooper pairs decreases these are expected to behave more and more like bosonic molecules and consequently a BEC should occur (see such transitions in optical lattices). The studies of this by Greiner et al. and on the crossover transition $\text{BCS} \rightleftharpoons \text{BEC}$ are of utmost interest [60]. For describing phase transitions (in optical lattices with sites i) one uses the Bose-Hubbard hamiltonian

$$H = - \sum_{i,j} t a_i^\dagger a_j + \sum_i (\epsilon_i - \mu) n_i + \frac{1}{2} \sum_i U n_i (n_i - 1).$$

Here, t denotes the hopping integral between (atomic) sites i , the chemical potential μ acts as a Lagrange multiplier and the interaction U between particles (atoms) tends to localize these. Note that triplet Cooper pairs do not show a BEC transition. Phase coherence of the Cooper pairs might affect the $\text{BCS} \rightarrow \text{BEC}$ transition. Coulomb interactions might suppress the pairing and cause a Mott transition.

Systems consisting of superconducting quantum dots may become very useful for quantum informa-

tion technology, see the review by Schön et al. [61]. The charge changes in Fig. 1.32 are due to Cooper pairs and describe the way to get two-level superconducting states [52,62]. Such quantum-state engineering using low capacitance Josephson tunneling junctions may yield quantum bits (qubits) for quantum information processing. As discussed by Schön et al. single-qubit and two-qubit quantum states can be controlled by gate voltage (or in the case of phase flux degrees of freedom by magnetic fields), see [62]. Applying Eq. (1.14) to the tunnel junction shown in Fig. 1.34 one has

$$H = 4E_c(n - n_g)^2 - E_J \cos \phi_{13} + \dots, \quad (1.24)$$

if for low capacitance and large superconducting gap energy Δ only tunneling of Cooper pairs occurs. E_c is the charging energy, n the number of extra Cooper pairs on system 3 ($n_{op} = -i\hbar\partial/\partial\hbar\phi$) and $n_g = C_g V_g/2e$ acts as a control parameter, see Fig 1.34. Here, we have applied a gate voltage V_g connecting an electrode to the superconductor 1 and another one that acts on the superconductor 3 via a gate capacitance C_g . This is a qubit yielding approximately a two-level system as illustrated in Fig. 1.36. A qubit with Cooper-pair states zero or one is similar to the 2 spin states ($|\uparrow\rangle = (10)$, $|\downarrow\rangle = (01)$) and may be described by the model Hamiltonian

$$H_Q = -\frac{1}{2} B_z \sigma_z - \frac{1}{2} B_x \sigma_x,$$

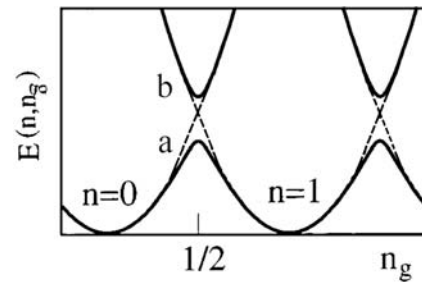


Fig. 1.36. Charging energy of superconducting electron box (see (3) in Fig. 1.34) as a function of a gate voltage $V_g(\alpha n_g)$. The degenerate parabola (dashed curves) split due to Josephson coupling mixing and one gets a two-level quantum system with states a , b and so on. The superconducting box (3) becomes a qubit with states $n = 0$, $n = 1$ similar to two spin-states

with $B_z \equiv 4E_c(1 - 2n_g)$ and $B_x \equiv E_J$. Combining several such systems (several tunnel junctions) one may achieve a behaviour that is useful for quantum-mechanical information technology [61, 62]. Interesting is also the case of a spin-polarized Josephson current (triplet superconductivity, a ferromagnetic medium 2, see Fig 1.34, etc.). A magnetic field could manipulate the tunnel current. If strong correlations occur in the tunnel medium (described by a Hubbard like Hamiltonian) then in particular irradiation may affect the electronic occupation of levels in the tun-

nel medium and thus manipulate the tunnel current (ultrafast switching).

Acknowledgements

We thank D. Manske, I. Eremin, F. Nogueira for helpful discussions and last but not least E. v. Sulzbach for encouragement. In particular we are also grateful to L. Tewordt, W. Buckel, R.D. Parks, M. Peter and B. Mühlischlegel for many discussions over the years.

References

1. H. Kamerlingh Onnes, Commun. Phys. Lab. Univ. Leiden, **120b,122b,124c**, (1911)
2. R.D. Parks, In: *Superconductivity*, Vols. 1, 2. Marcel Dekker, New York (1969); J.R. Schrieffer, *Theory of Superconductivity* (Benjamin, New York, 1964)
3. K. Shimizu et al., Nature **412**, 316 (2001)
4. J.G. Bednorz and K.A. Müller, Z. Phys. B **64**, 189 (1986)
5. W. Meissner, R. Ochsenfeld, Naturwissenschaften **21**, 787 (1933)
6. F. London and H. London, Proc. Roy. Soc. (London), A **149**, 71 (1935); Physica A **2**, 341 (1935)
7. E. Maxwell, Phys. Rev. B **78**, 477 (1950)
8. V.L. Ginzburg, L.D. Landau, Zh.Eksp. Teor. Fiz. **20**, 1064 (1960)
9. J. Bardeen, L.N. Cooper, J.R. Schrieffer, Phys. Rev. B **108**, 1175 (1957)
10. L.P. Gor'kov, Zh. Eksp. Teor. Fiz. **36**, 1918 (1958); Sov. Phys. JETP **9**, 1364 (1958)
11. A.A. Abrikosov, L.P. Gor'kov, I.E. Dzyaloshinskii, In: *Methods of Quantum Field Theory in Statistical Mechanics* (Prentice Hall, Englewood Cliffs, NJ, 1963)
12. G.M. Eliashberg, JETP **11**, 696 (1960)
13. A.A. Abrikosov, Sov. Phys. JETP **5**, 1174 (1957)
14. B.D. Josephson, Phys. Lett. **1**, 251 (1962)
15. J.R. Schrieffer, D.J. Scalapino, J.W. Wilkens, Phys. Rev. Lett. **10**, 336 (1963)
16. R. Doll and M. Näbauer, Phys. Rev. Lett. **7**, 51 (1961); B.D. Deaver and W.M. Fairbank, Phys. Rev. Lett. **7**, 43 (1961)
17. W.L. McMillan, Phys. Rev. **167**, 331 (1968)
18. P.B. Allen In: *Dynamical Properties of Solids*, Vol. 3, ed. by G.K. Horton et al. (North Holland, Amsterdam, 1980) p. 95; G. Bergmann and D. Rainer, Z. Physik **263**, 59 (1973)
19. D. Osheroff, R.C. Richardson, D.M. Lee, Phys. Rev. Lett. **28**, 885 (1972); for reviews see *The Physics of Liquid and Solid Helium* K.H. Bennemann, and J.B. Ketterson, Eds. (Wiley, New York, 1978)
20. N.F. Berk, J.R. Schrieffer, Phys. Rev. Lett. **17**, 433 (1966); Phys. Rev. B **30**, 1408 (1966)
21. L. Degiorgi, Rev. Mod. Phys. **71**, 687 (1999); F. Steglich et al., J. Phys. Chem. Sol. **59**, 2190 (1998); F. Steglich et al. Physica C **341-348**, 691 (2000)
22. J.L. Tallon, Phys. Rev. B **51**, 12911 (1995); D. Manske, K.H. Bennemann, Physica C **341-348**, 83 (2000)
23. C.C. Tsuei, J.R. Kirtley, Rev. of Modern Physics **72**, 969 (2000)
24. D. Manske, T. Dahm, and K.H. Bennemann, Phys. Rev. B **64**, 144520 (2001)
25. A.J. Millis, H. Monien, D. Pines, Phys. Rev. B **42**, 167 (1990)
26. V. Emery, S.A. Kivelson, Physica C **209**, 597 (1993)
27. T. Dahm and L. Tewordt, Phys. Rev. Lett. **74**, 793 (1995)
28. M. Langer, J. Schmalian, S. Grabowski, and K.H. Bennemann, Phys. Rev. Lett. **75**, 4508 (1995)
29. N.E. Bickers and D.J. Scalapino, Annals of Physics **193**, 206 (1989)
30. D.J. Scalapino, Phys. Rep. **250**, 329 (1995)

31. J. Schmalian, M. Langer, S. Grabowski, and K.H. Bennemann, *Comp. Phys. Comm.* **93**, 141 (1996)
32. D. Manske, I. Eremin, and K.H. Bennemann, *Phys. Rev. B* **63**, 054517 (2001); D. Manske and K.H. Bennemann, *Mol. Phys. Rep.* **24**, 52 (1999); D. Manske, I. Eremin, and K.H. Bennemann, *Phys. Rev. B* **62**, 13922 (2000); I. Eremin, D. Manske, C. Joas, and K.H. Bennemann, cond-mat 0102074; D. Manske and K.H. Bennemann, In: *Fluctuating Paths and Fields*, ed. W. Janke et al. (World Scientific, Singapore, 2001)
33. P. Bourges, In: *Gap Symmetry and Fluctuations in High-Tc Superconductors*, eds. J. Bok, G. Deutscher, D. Pavuna and S. Wolf (Plenum Press, New York, 1998)
34. C.C. Tsuei, and J.R. Kirtley, *Phys. Rev. Lett.* **85**, 182 (2000)
35. K. Ishida, H. Mukuda, Y. Kitaoka, Z.Q. Mao, H. Fukuzawa, and Y. Maeno, *Phys. Rev. B* **63**, 060507 (2001)
36. Y. Maeno et al., *Nature* **372**, 532 (1994)
37. Y. Maeno, T.M. Rice, M. Sigrist, *Physics Today* **42-47**, (2001)
38. Y. Maeno et al, *Nature* **372**, 532 (1994); T.M. Rice, *Nature* **396**, 627 (1998); Y. Maeno, T.M. Rice, M. Sigrist, *Physics Today* **54**, 42, *Physica C* **341-348** 695 (2000)
39. J. Nagamatsu, N. Nakagawa, T. Musanaka, Y. Zenitana, J. Akimitsu, *Nature* **410**, 63 (2001)
40. D. Manske, I. Eremin, and K.H. Bennemann, In: *The Physics of Superconductors*, Vol 2 (Springer, 2003)
41. A. Mackenzie, Y. Maeno and S. Julian, *Phys. World* **15** (No. 4), 33 (2002)
42. M.B. Maple, *Physica C* **341-348**, 47 (2000)
43. H.v. Löhneysen, *Physica B* **197**, 551 (1994); N.D. Mathur et al., *Nature* **394**, 39 (1998)
44. H.R. Ott, In: *The Physics of Superconductors Vol. 1*, Eds. K.H. Bennemann, J.B. Ketterson (Springer, 2002)
45. L. Degiorgi, *Rev. Mod. Phys.* **71** 687 (1999); F. Steglich et al. *J. Phys. Chem. Sol.* **59**, 2190 (1998); M.B. Maple, *Physica C* **341-348**, 47 (2000); C.R. Stewart, *Rev. of Mod. Physics* **73**, 797 (2001); R. Joynt and L. Taillefer, *Rev. Mod. Phys.* **74**, 235 (2002)
46. M. Vojta, *Phys. Bl.* **55**, March 2002; S. Sachdev: *Quantum Phase Transitions* (Cambridge Univ. Press, 1999); J. Flouquet and A. Buzdin, *Phys. World* **15**, 41(2002)
47. A.I. Larkin, Yu.N. Ovchinnikov, *JETP* **20**, 762 (1965)
48. J. Singleton and C. Mielke, *Phys. World* **15** (No1) 35 (2002); T. Ishiguo et al., *Organic Superconductors* (Springer 1998); M. Lang, In: *The Physics of Superconductors Vol. 2*, Eds. K.H. Bennemann, J.B. Ketterson (Springer, 2003)
49. J.W. Garland, K.H. Bennemann, F.M. Mueller, *Phys. Rev. Lett.* **21**, 1315 (1968); W. Buckel, and R. Hilsch, *Z. Phys.* **138**, 109 (1954)
50. K.H. Bennemann, *Z. Physik* **260**, 367 (1973)
51. W. Belzig and C. Bruder, *Phys. Bl.* **56** (No.5) 35 (2000); C.W.J. Beenakker, In: *Mesoscopic Quantum Physics* (North Holland, Amsterdam 1995); B. Mühschlegel, *Surface Rev. and Lett.* **3** (No.1) 115 (1996); W.P. Halperin, *Rev. Mod. Phys.* **58**, 533 (1986); B. Janko, L. Smith, V. Ambegaokar, *Phys. Rev. B* **50**, 1152; M.T. Tuominen, J.M. Hergenrother, T.S. Tighe, and M. Tinkham, *Phys. Rev. Lett.* **69** (1992) 1997; *Mesoscopic Superconductivity Physica B* **203**, 201 (1994); Y. Imry, *Introduction to Mesoscopic Physics* (Oxford Univ. Press, 1997); B.L. Altshuler et al., *Mesoscopic Phenomena in Solids* (North-Holland, Amsterdam 1991)
52. J.B. Ketterson and S.N. Long, *Superconductivity* (Cambridge Univ. Press, 1999)
53. F.S. Nogueira and K.H. Bennemann, *Europhys. Lett.* **67**, 620 (2004)
54. I. Baladić, A. Buzdin, N. Ryzhanova and A. Vedyayev, *Phys. Rev. B* **63**, 54518 (2001); Y. Asano, Y. Tanaka, M. Sigrist, and S. Kashiwaya, cond-mat /0212353v1
55. L.B. Ioffe and M.V. Feigel'man, cond-mat /0203011; B. Doucot, M.V. Feigel'man and L.B. Ioffe, *Phys. Rev. Lett.* **90**, 107003 (2003)
56. B. Kastening, D. Morr, D. Manske, and K. Bennemann, *Phys. Rev. Lett.* **96**, 47009 (2006)
57. C.C. Homes, *Nature* **430**, 539–541 (2004); T. Timusk, *Physics World* **18**, p. 31, (2005)
58. T. Takada, H. Sakurai, E. Takayama-Muromachi, F. Izumi, R.A. Dilanian, and T. Sasaki, *Nature* **422**, 53 (2003)
59. E. Babaev, A. Sudbo, N.W. Ashcroft, *Nature* **431**, 666 (2004)
60. M. Greiner, I. Bloch, O. Mandel, T. Hänsch, T. Esslinger, *Phys. Rev. Lett.* **87**, 160405 (2001), M. Greiner et al., *Nature* **415**, 39 (2002); C.A. Regal, M. Greiner, D.S. Jin, *Phys. Rev. Lett.* **92**, 40403 (2004)
61. Y. Makhlim, G. Schön, A. Shnirman, *Rev. Mod. Phys.* **73**, 357 (2001)
62. M. Trinklham, *Introduction to Superconductivity* (Dover, Mineola, NY, 1996)

Superconductivity

Volume 1: Conventional and Unconventional

Superconductors Volume 2: Novel Superconductors

Bennemann, K.-H.; Ketterson, J.B. (Eds.)

2008, XXXII, 1568 p. In 2 volumes, not available
separately., Hardcover

ISBN: 978-3-540-73252-5